

ASYMPTOTIC BEHAVIOUR OF THE FIFTH PAINLEVÉ TRANSCENDENTS IN THE SPACE OF INITIAL VALUES

NALINI JOSHI AND MILENA RADNOVIĆ

ABSTRACT. We study the asymptotic behaviour of the solutions of the fifth Painlevé equation as the independent variable approaches zero and infinity in the space of initial values. We show that the limit set of each solution is compact and connected and, moreover, that any solution with the essential singularity at zero has an infinite number of poles and zeroes, and any solution with the essential singularity at infinity has infinite number of poles and takes value 1 infinitely many times.

CONTENTS

1. Introduction	1
2. The space of initial values	2
2.1. A system equivalent to P_V	3
2.2. The autonomous equation	3
2.3. Resolution of singularities	4
2.4. Movable singularities in Okamoto's space	6
3. Special solutions	7
3.1. Special solutions and singular conics	7
3.2. Other special solutions of P_V	9
4. The solutions near the infinity set	9
5. The limit set	16
6. Limit $x \rightarrow \infty$	17
Appendix A. Resolution of the system	18
A.1. The affine charts	18
A.2. Blow ups	19
Appendix B. Notation	28
References	29

1. INTRODUCTION

Following the construction of initial value spaces of Painlevé equations by Okamoto (1979), and more recent asymptotic analysis of the solutions of the first, second and fourth Painlevé equations in such spaces, we investigate the solutions of the fifth Painlevé equation:

$$(1.1) \quad P_V : \frac{d^2 y}{dx^2} = \left(\frac{1}{2y} + \frac{1}{y-1} \right) \left(\frac{dy}{dx} \right)^2 - \frac{1}{x} \frac{dy}{dx} + \frac{(y-1)^2}{x^2} \left(\alpha y + \frac{\beta}{y} \right) + \frac{\gamma y}{x} + \frac{\delta y(y+1)}{y-1},$$

This research was supported by an Australian Laureate Fellowship # FL120100094 from the Australian Research Council. The research of M.R. was partially supported by the Serbian Ministry of Education and Science (Project no. 174020: Geometry and Topology of Manifolds and Integrable Dynamical Systems).

in an asymptotic limit in its initial value space. Complete information about the limit sets of transcendental solutions and their behaviours near the infinity set are found. Unlike earlier asymptotic investigations of P_V , we do not impose any reality constraints; here y is a function of the complex variable x , and $\alpha, \beta, \gamma, \delta$ are given complex constants.

Noting that P_V has (fixed) essential singularities only when the independent variable x takes the values 0 and ∞ , we investigate the behaviour of the solutions near $x = 0$. A similar analysis can be carried out near ∞ and we also include an outline of the main results for this limit. We show that each solution that is singular at $x = 0$ has infinitely many poles and zeroes in every neighbourhood of this point. Similarly, each solution singular at $x = \infty$ has infinitely many poles and, moreover, takes the value 1 infinitely many times in each neighbourhood of infinity.

The starting point for our analysis is the compactification and regularisation of the initial-value space. To make explicit analytic estimates possible, we calculate detailed information about the Painlevé vector field after each resolution (or blow-up) of this space. A similar approach was carried out for the first, second, and fourth Painlevé equations respectively by Duistermaat and Joshi (2011), Howes and Joshi (2014), and Joshi and Radnović (2016). However, the construction of the initial-value spaces in each of these earlier works consisted of exactly nine blow-ups, while in the present paper, we will see that eleven blow-ups are needed, followed by two blow-downs.

The asymptotic analysis of the fifth Painlevé transcendent has been studied by many authors, including Andreev and Kitaev (1997a, 1997b, 2000), Zeng and Zhao (2016), Bryuno and Parusnikova (2006), Qin and Shang (2006), Lu and McLeod (1999a, 1999b), McCoy and Tang (1986a, 1986b, 1986c), Jimbo (1982). However, the literature on the asymptotic behaviours of the fifth Painlevé transcendent concentrates on behaviours on the real line, often focusing on special behaviours or solutions, while we consider all solution behaviours for $x \in \mathbb{C}$. For other mathematical results related to P_V , see (Boelen et al., 2013; Shimomura, 2011; Kaneko and Ohyama, 2007; Sasaki, 2007; Clarkson, 2005; Lu and Shao, 2004; Gordoa et al., 2001a; 2001b), while for applications in physics see (Jimbo et al., 1980; Dyson, 1995; Schief, 1994), and references therein.

This paper is organised as follows. In Section 2, we construct and describe the space of the initial values for equation (1.1), with complete details of all the necessary calculations provided in Appendix A. In Section 3, we consider the special solutions of P_V . Section 4 contains the analysis of the behaviours of solutions near the infinity set in the space of initial values. Results on the complex limit sets of solutions when the independent variable approaches 0 are provided in Section 5. The behaviours of the fifth Painlevé transcendent in the limit $x \rightarrow \infty$ are outlined in Section 6. A summary of the notation used in this paper is given in Appendix B.

2. THE SPACE OF INITIAL VALUES

Since the fifth Painlevé equation is a second-order differential equation, solutions are locally defined by two initial values. Therefore the space of initial values is two complex-dimensional. However, standard existence and uniqueness theorems only cover values of y that are not arbitrarily close to 0, 1 or infinity (where the second derivative given by P_V becomes ill-defined). To compactify and regularize the space of initial values to cover all possible initial values, we start by converting P_V to an equivalent system of two first-order equations, which is convenient for studying the limit $x \rightarrow 0$; see Section 2.1. We discuss the corresponding autonomous system in Section 2.2. In Section 2.3, we construct the space of initial values and its compactification in the limit $x \rightarrow 0$.

In this space, the series expansions of solutions of P_V near singular y -values become regular expansions. In Section 2.4, we provide the singular expansions of the solutions in neighbourhoods where y becomes arbitrarily close to the values 0, 1, ∞ and give the corresponding regularized Taylor expansions of solutions near the corresponding exceptional lines in the initial value space.

2.1. **A system equivalent to P_V .** With the change of the independent variable $t = \log x$, Equation (1.1) becomes:

$$(2.1) \quad \begin{aligned} \frac{d^2 y}{dt^2} &= \left(\frac{1}{2y} + \frac{1}{y-1} \right) \left(\frac{dy}{dt} \right)^2 + (y-1)^2 \left(\alpha y + \frac{\beta}{y} \right) \\ &\quad + e^t \gamma y + e^{2t} \frac{\delta y(y+1)}{y-1}. \end{aligned}$$

We rewrite Equation (2.1) in the following way:

$$(2.2) \quad \begin{aligned} \frac{dy}{dt} &= 2y(y-1)^2 z - (\theta_0 + \eta)y^2 + (2\theta_0 + \eta - \theta_1 e^t)y - \theta_0, \\ \frac{dz}{dt} &= -(y-1)(3y-1)z^2 + (2(\theta_0 + \eta)y - 2\theta_0 - \eta + \theta_1 e^t)z \\ &\quad - \frac{1}{2}\epsilon(\theta_0 + \eta - \theta_\infty), \end{aligned}$$

where $\theta_\infty^2 = 2\alpha$, $\theta_0^2 = -2\beta$, $\theta_1^2 = -2\delta$ ($\theta_1 \neq 0$), $\eta = -\frac{\gamma}{\theta_1} - 1$, and $\epsilon = \frac{1}{2}(\theta_0 + \theta_\infty + \eta)$.

Remark 2.1. Here, we assumed that $\delta \neq 0$, which is a generic case of the fifth Painlevé equation. When $\delta = 0$, the P_V is equivalent to the third Painlevé equation (Ohyama and Okumura, 2006).

The system (2.2) is Hamiltonian:

$$\frac{dy}{dt} = \frac{\partial H}{\partial z}, \quad \frac{dz}{dt} = -\frac{\partial H}{\partial y},$$

with Hamiltonian function:

$$(2.3) \quad H = y(y-1)^2 z^2 - (\theta_0 + \eta)y^2 z + (2\theta_0 + \eta - \theta_1 e^t)yz - \theta_0 z + \frac{1}{2}\epsilon(\theta_0 + \eta - \theta_\infty)y.$$

2.2. **The autonomous equation.** The autonomous equation corresponding to (2.1) is:

$$(2.4) \quad \frac{d^2 y}{dt^2} = \left(\frac{1}{2y} + \frac{1}{y-1} \right) \left(\frac{dy}{dt} \right)^2 + (y-1)^2 \left(\alpha y + \frac{\beta}{y} \right),$$

which is equivalent to the autonomous version of (2.2):

$$(2.5) \quad \begin{aligned} \frac{dy}{dt} &= (y-1)^2(2yz - \theta_0) + \eta y(y-1), \\ \frac{dz}{dt} &= (y-1)z(2\eta + 2\theta_0 + z - 3yz) + \eta z - \frac{1}{2}\epsilon(\theta_0 + \eta - \theta_\infty). \end{aligned}$$

System (2.5) is also Hamiltonian:

$$\frac{dy}{dt} = \frac{\partial E}{\partial z}, \quad \frac{dz}{dt} = -\frac{\partial E}{\partial y},$$

with Hamiltonian:

$$(2.6) \quad E = y(y-1)^2 z^2 - (\theta_0 + \eta)y^2 z + (2\theta_0 + \eta)yz - \theta_0 z + \frac{1}{2}\epsilon(\theta_0 + \eta - \theta_\infty)y.$$

Using the first equation of (2.5) to express z , and using the fact that E is constant along solutions, we get:

$$\left(\frac{dy}{dt} \right)^2 = (y-1)^2(4Cy + \theta_0^2 - 2\theta_0(\eta + \theta_0)y + \theta_\infty^2 y^2), \quad C = \text{const.}$$

It is worth observing that the constant function $y \equiv 1$ is the only solution of this equation taking the value 1. From (2.5), the corresponding function z is the solution of

$$\frac{dz}{dt} = \eta z - \frac{1}{2}\epsilon(\theta_0 + \eta - \theta_\infty).$$

That is, we have

$$z = c_1 e^{\eta t} + \frac{\epsilon(\theta_0 + \eta - \theta_\infty)}{2\eta},$$

where c_1 is a constant.

The flow (2.5) has four fixed points:

$$(y, z) = \begin{cases} \left(1, \frac{\epsilon(\theta_0 + \eta - \theta_\infty)}{2\eta}\right) \\ \left(Y_i, \frac{\theta_0}{2Y_i} + \frac{\eta}{2(1 - Y_i)}\right), i \in \{1, 2, 3\}, \end{cases}$$

where Y_1, Y_2, Y_3 are the roots of the following cubic polynomial in Y :

$$\begin{aligned} &(-\theta_\infty^2 - 6\eta^2 + 8\eta\theta_0 + 2\theta_0^2) Y^3 \\ &+ (2\eta^2 - 12\eta\theta_0 - 2\theta_0^2 + \theta_\infty^2) Y^2 + \theta_0(4\eta - \theta_0)Y + \theta_0^2. \end{aligned}$$

We display the intersection diagram of the space of initial values \mathcal{F}_∞ of the autonomous system (2.5) in Figure 1, to provide a comparison with the construction of the initial value space of the non-autonomous system (2.2) provided in the next subsection. \mathcal{F}_∞ is constructed

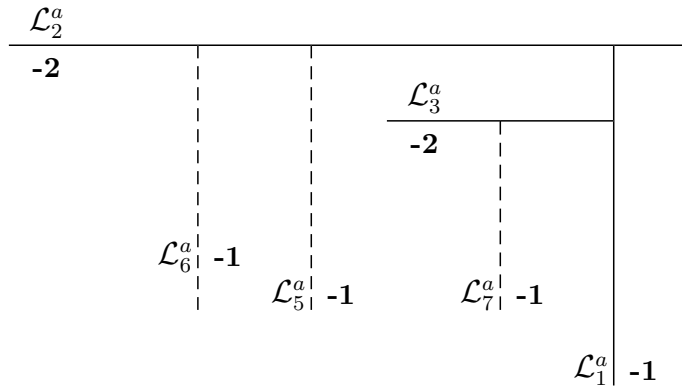


FIGURE 1. The space \mathcal{F}_∞ of initial values of the autonomous system (2.5).

by a sequence of blow-ups, carried out along the lines of the construction of the space of the initial values for the non-autonomous system (2.2). For those readers who may wish to carry this out separately, we note that the point a_4 (found in Section A.2.2) will be a base point only for the non-autonomous system.

2.3. Resolution of singularities. The explicit resolution of the vector field (2.2) is carried out in Appendix A. As mentioned above, the process requires 11 resolutions of singularities, or, blow-ups.

The fiber (or intersection diagram) $\mathcal{F}(t)$ of the resulting Okamoto space is shown in Figure 2. Note that in this figure, \mathcal{L}_∞^* is the proper preimage of the line at the infinity, while $\mathcal{L}_0^*, \mathcal{L}_1^*, \mathcal{L}_2^*, \mathcal{L}_3^*, \mathcal{L}_4^*, \mathcal{L}_8^*, \mathcal{L}_9(t)^*$ are proper preimages of exceptional lines obtained by blow ups at points $a_0, a_1, a_2, a_3, a_4, a_8, a_9$ respectively and $\mathcal{L}_5, \mathcal{L}_6, \mathcal{L}_7, \mathcal{L}_{10}(t)$ are exceptional lines obtained by blowing up points a_5, a_6, a_7, a_{10} respectively. The self-intersection number of each line (after all blow-ups are completed) is indicated in the figure.

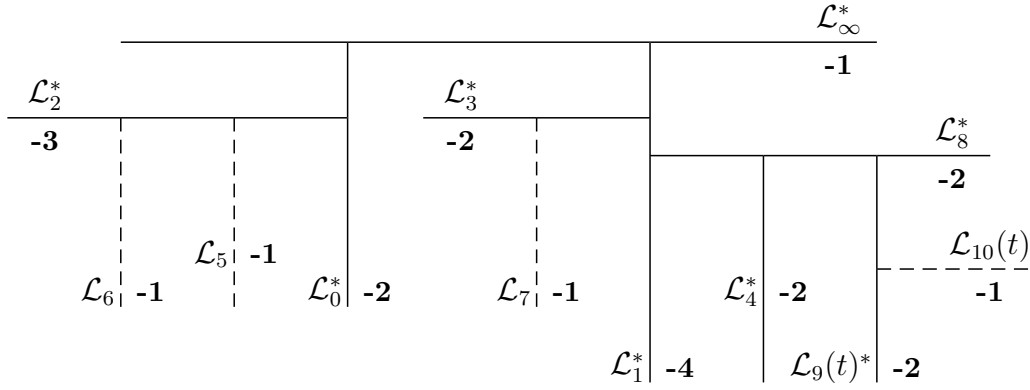


FIGURE 2. The fiber $\mathcal{F}(t)$ of the Okamoto space.

Each line with self-intersection number -1 can be blown down again. Blowing down \mathcal{L}_∞^* and then the projection of \mathcal{L}_0^* , we get another representation of the fiber $\mathcal{F}(t)$, which is shown in Figure 3. The projection of each remaining line in Figure 2 is denoted by the same index but now with superscript p . Notice that the self-intersection numbers of \mathcal{L}_1^p and \mathcal{L}_2^p are no longer the same as the corresponding pre-images \mathcal{L}_1^* and \mathcal{L}_2^* in Figure 2. In this space, we denote by \mathcal{I} the set where the vector field associated to (2.2) is infinite:

$$\mathcal{I} = \bigcup_{j=0}^4 \mathcal{L}_j^p \cup \mathcal{L}_8^p \cup \mathcal{L}_9^p.$$

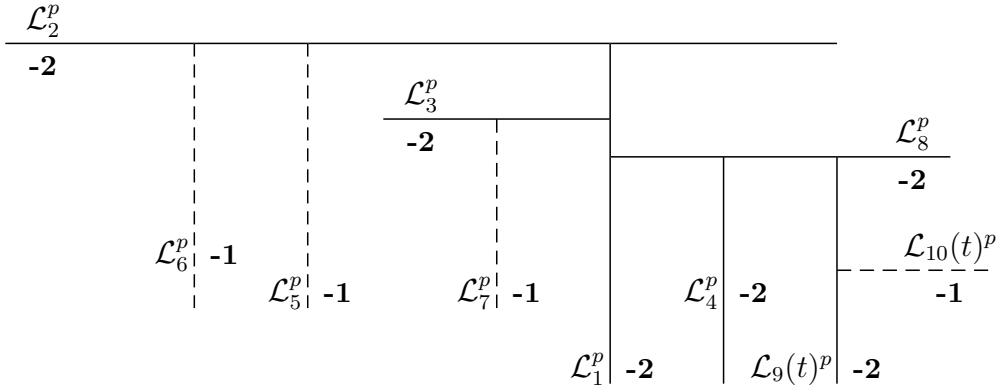
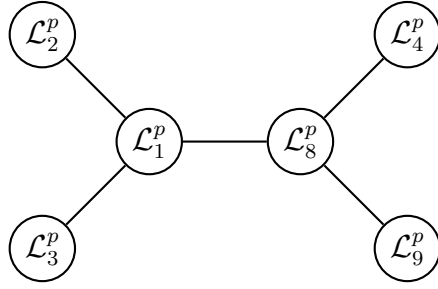


FIGURE 3. The fiber $\mathcal{F}(t)$ of the Okamoto space, after two blow downs.

Well-known correspondences in algebraic geometry show that the lines of self-intersection -2 can be interpreted as simple roots in an affine Weyl group. Representing each such line by a node and connecting a pair of nodes by a line only if they intersect in the fibre, we obtain the Dynkin diagram shown in Figure 4, which is of type $D_5^{(1)}$.

FIGURE 4. The Dynkin diagram of $D_5^{(1)}$.

In the limit $\text{Re } t \rightarrow -\infty$, the resulting Okamoto space is compactified by the fiber \mathcal{F}_∞ , corresponding to the autonomous system (2.5), see Figure 1. Its infinity set is given by

$$\mathcal{I}_\infty = \mathcal{L}_1^a \cup \mathcal{L}_2^a \cup \mathcal{L}_3^a.$$

2.4. Movable singularities in Okamoto's space. Here, we consider neighbourhoods of exceptional lines where the Painlevé vector field (2.2) becomes unbounded. The construction given in Appendix A shows that these are given by the lines \mathcal{L}_5 , \mathcal{L}_6 , \mathcal{L}_7 and \mathcal{L}_{10} .

Movable pole with residue $-\theta_\infty$. The set $\mathcal{L}_5 \setminus \mathcal{I}$ is given by $y_{62} = 0$ in the (y_{62}, z_{62}) chart. Suppose $y_{62}(\tau) = 0$, $z_{62}(\tau) = B$, for arbitrary complex numbers τ , B . Solving the system of differential equations for y_{62} , z_{62} in Section A.2.6 in a neighbourhood of $t = \tau$, we obtain

$$y_{62} = -\theta_\infty(t - \tau) + \frac{\theta_\infty}{2}(2B - 2\theta_\infty - \eta - \theta_1 e^\tau)(t - \tau)^2 + O((t - \tau)^3).$$

Since the transformation from (y_{62}, z_{62}) to (y, z) (also given in Section A.2.6) is

$$y = \frac{1}{y_{62}} \quad \text{and} \quad z = y_{62}(y_{62}z_{62} + 1),$$

we obtain series expansions for (y, z) given by

$$\begin{aligned} y &= -\frac{\theta_\infty}{t - \tau} - \frac{2B - 2\theta_\infty - \eta - \theta_1 e^\tau}{2\theta_\infty} + O(t - \tau), \\ z &= -\theta_\infty(t - \tau) + \frac{\theta_\infty}{2}(2B(1 + \theta_\infty) - \eta - 2\theta_\infty - \theta_1 e^\tau)(t - \tau)^2 \\ &\quad + O((t - \tau)^3). \end{aligned}$$

Clearly, y has a simple pole with residue $-\theta_\infty$, while z has a simple zero at $t = \tau$.

Movable pole with residue θ_∞ . At the intersection with $\mathcal{L}_6 \setminus \mathcal{I}$, y has a simple pole with the residue θ_∞ , while z has a simple zero. This case is analogous to the previous one, see Sections A.2.6 and A.2.7.

Movable zero with coefficient θ_0 . The set $\mathcal{L}_7 \setminus \mathcal{I}$ is given by $z_{81} = 0$ in the (y_{81}, z_{81}) chart. Suppose $y_{81}(\tau) = B$ and $z_{81}(\tau) = 0$. Then integration of the vector field gives

$$\begin{aligned} z_{81}(t) &= (t - \tau) + \frac{\eta - 2\theta_0 - \theta_1 e^\tau}{2}(t - \tau)^2 \\ &\quad + \frac{F - 2\eta\theta_0 + \theta_0^2 - \theta_1 e^\tau - 4B}{3}(t - \tau)^3 + O((t - \tau)^4). \end{aligned}$$

Since

$$y = z_{81}(y_{81}z_{81} + \theta_0), \quad z = \frac{1}{z_{81}},$$

we obtain

$$\begin{aligned} y &= \theta_0(t - \tau) + \frac{2B + \theta_0(\eta - 2\theta_0 - \theta_1 e^\tau)}{2}(t - \tau)^2 + O((t - \tau)^3), \\ z &= \frac{1}{t - \tau} - \frac{\eta - 2\theta_0 - \theta_1 e^\tau}{2} \\ &\quad + \left(\frac{(\eta - 2\theta_0 - \theta_1 e^\tau)^2}{4} - \frac{F - 2\eta\theta_0 + \theta_0^2 - \theta_1 e^\tau - 4B}{3} \right) (t - \tau) \\ &\quad + O((t - \tau)^2). \end{aligned}$$

Thus, y has a simple zero and z a simple pole at $t = \tau$.

Movable points where y becomes unity. The set $\mathcal{L}_{10} \setminus \mathcal{I}$ is given by $z_{111} = 0$ in the (y_{111}, z_{111}) chart. Suppose $y_{111}(\tau) = B$ and $z_{111}(\tau) = 0$. Then

$$\begin{aligned} z_{111} &= (t - \tau) + \frac{\theta_1 e^\tau - \eta - 1}{2}(t - \tau)^2 \\ &\quad + \frac{1}{3} \left(1 + \frac{5}{2}\eta + \eta^2 - \frac{B}{\theta_1 e^\tau} + \theta_1 e^\tau \left(1 - \theta_0 - \frac{\eta}{2} \right) + \frac{1}{2}\theta_1^2 e^{2\tau} \right) (t - \tau)^3 \\ &\quad + O((t - \tau)^4). \end{aligned}$$

Since we have

$$\begin{aligned} y &= 1 + \theta_1 e^t z_{111} + (1 + \eta)\theta_1 e^t z_{111}^2 + y_{111} z_{111}^3, \\ z &= \frac{1}{z_{111}^2(\theta_1 e^t + (1 + \eta)\theta_1 e^t z_{111} + y_{111} z_{111}^2)}, \end{aligned}$$

it follows that $y(\tau) = 1$ and z has a double pole at $t = \tau$. Their expansions around this point are given by

$$\begin{aligned} y &= 1 + \theta_1 e^\tau (t - \tau) + \frac{\theta_1 e^\tau (\theta_1 e^\tau + \eta + 3)}{2}(t - \tau)^2 \\ &\quad + \frac{\theta_1 e^\tau}{6} \left(2 - 4\eta - 4\eta^2 - \frac{2B}{\theta_1 e^\tau} + (11 + 5\eta - 2\theta_0)\theta_1 e^\tau + \theta_1^2 e^{2\tau} \right) (t - \tau)^3 \\ &\quad + O((t - \tau)^4), \\ z &= \frac{(\theta_1 e^\tau)^{-1}}{(t - \tau)^2} + \frac{1 + (\theta_1 e^\tau)^{-1}}{t - \tau} + \left(\frac{2B}{\theta_1 e^\tau} + \frac{\eta\theta_1 e^\tau}{2} + \theta_0\theta_1 e^\tau + \frac{\theta_1^2 e^{2\tau}}{4} - \frac{1 + 3\eta^2}{4} \right) \\ &\quad + O(1). \end{aligned}$$

3. SPECIAL SOLUTIONS

In this section, we consider the pencil of curves corresponding to the Hamiltonian (2.6) of the autonomous system (2.5). We show that by a birational equivalence, this pencil can be transformed to a pencil of conics. In Section 3.1, we analyse the solutions of the fifth Painlevé equation corresponding to singular conics from the pencil. In Section 3.2, we give a summary of other special solutions.

3.1. Special solutions and singular conics. The pencil of curves arising from the Hamiltonian of the autonomous system (2.5) is given by the zero set of the one-parameter family of polynomials (parametrised by c):

$$\begin{aligned} (3.1) \quad h_c(y, z) &= y(y - 1)^2 z^2 - (\theta_0 + \eta)y^2 z + (2\theta_0 + \eta)yz - \theta_0 z \\ &\quad + \frac{1}{2}\epsilon(\theta_0 + \eta - \theta_\infty)y - c. \end{aligned}$$

For each c , the curve $h_c(y, z) = 0$ is birationally equivalent to

$$h_{\tilde{c}}^1(y_1, z_1) = \frac{z_1^2 - (\theta_0^2 + \tilde{c}y_1 + \theta_\infty^2 y_1^2)}{4y_1} = 0,$$

where $\tilde{c} = 4c - 2\theta_0(\eta + \theta_0)$ and the birational equivalence is given by

$$y_1 = y, \quad z_1 = 2y(y-1)z - (\theta_0 + \eta)y + \theta_0.$$

The family of level curves $h_{\tilde{c}}^1 = 0$ forms a pencil of conics. The singular conics in the pencil are:

$$\begin{aligned} \tilde{c} = 2\theta_0\theta_\infty, & \quad (z_1 + \theta_\infty y_1 + \theta_0)(z_1 - \theta_\infty y_1 - \theta_0) = 0, \\ \tilde{c} = -2\theta_0\theta_\infty, & \quad (z_1 - \theta_\infty y_1 + \theta_0)(z_1 + \theta_\infty y_1 - \theta_0) = 0, \\ \tilde{c} = \infty, & \quad y_1 w_1 = 0, \end{aligned}$$

where $[y_1 : z_1 : w_1]$ are homogeneous coordinates. Moreover, the base points of this pencil are:

$$[0 : \theta_0 : 1], \quad [0 : -\theta_0 : 1], \quad [1 : \theta_\infty : 0], \quad [1 : -\theta_\infty : 0].$$

Recalling that the Hamiltonian E of the autonomous system, given by Equation (2.6), has the time derivative

$$E' = -\theta_1 e^t (z(2\theta_0 - (\eta + 2\theta_0)y + 2y(y-1)z) + E),$$

we can also search for conditions under which all successive derivatives of E are zero. This happens if and only if

$$z = 0 \quad \text{or} \quad 2\theta_0 - (\eta + 2\theta_0)y + 2y(y-1)z = 0.$$

These cases are investigated in further detail below.

Case $z = 0$. From the second equation of (2.2) we have $\epsilon(\theta_0 + \eta - \theta_\infty) = 0$, i.e. $\theta_0 + \eta = \pm\theta_\infty$. In this case $z_1 = \pm\theta_\infty y_1 + \theta_0$, and so this case corresponds to lines in the pencil of conics containing the base point $[0 : \theta_0 : 1]$.

The first equation of (2.2) is then a Riccati equation:

$$\frac{dy}{dt} = \mp\theta_\infty y^2 + (\theta_0 \pm \theta_\infty - \theta_1 e^t)y - \theta_0,$$

which is equivalent to

$$(3.2) \quad x \frac{dy}{dx} = \mp\theta_\infty y^2 + (\theta_0 \pm \theta_\infty - \theta_1 x)y - \theta_0.$$

For $\theta_\infty \theta_1 \neq 0$, the solutions of this equation can be expressed in terms of the Whittaker functions (Olver et al., 2010). Note that $\theta_1 \neq 0$ is equivalent to $\delta \neq 0$, when the P_V can be renormalised to $\delta = -1/2$. Then, the solutions of (3.2) are given by

$$y = -\frac{z\phi'(x)}{\theta_\infty\phi(x)},$$

where

$$\phi(x) = \frac{C_1 M_{\kappa, \mu}(\xi) + C_2 W_{\kappa, \mu}(\xi)}{\xi^\kappa} e^{\xi/2},$$

with $\xi = \pm x$, $\kappa = (\mp\theta_\infty - \theta_0 + 1)/2$, $\mu = \mp\theta_\infty + \theta_0$, and C_1, C_2 being arbitrary constants.

Solutions from this class intersect only the pole lines \mathcal{L}_5 and \mathcal{L}_6 .

Case $2\theta_0 - (\eta + 2\theta_0)y + 2y(y - 1)z = 0$. The first equation of (2.2) is then:

$$\frac{dy}{dt} = \theta_0 y^2 - (2\theta_0 + \theta_1 e^t)y + \theta_0,$$

which is again a Riccati equation that can be solved analogously to the previous case of (3.2). Since in this case $z_1 = \theta_0 y - \theta_0$, the condition on the constants is $\theta_0 = \pm\theta_\infty$. The solutions belong to the lines from the pencil of conics that contain the base point $[0 : -\theta_0 : 1]$.

Solutions from this class intersect only the pole line \mathcal{L}_7 .

3.2. Other special solutions of P_V . All rational solutions of P_V are of the form

$$y = \lambda x + \mu + \frac{P(x)}{Q(x)},$$

where λ, μ are constants and P, Q polynomials of degrees $n - 1$ and n respectively.

Such solutions can be obtained by applying Bäcklund transformations:

$$\begin{aligned} \mathcal{S}_1 &: (y(x); \alpha, \beta, \gamma, \delta) \mapsto (y(-x); \alpha, \beta, -\gamma, \delta), \\ \mathcal{S}_2 &: (y(x); \alpha, \beta, \gamma, \delta) \mapsto \left(\frac{1}{y(x)}; -\beta, -\alpha, -\gamma, \delta \right), \\ \mathcal{T}_{\varepsilon_1, \varepsilon_2, \varepsilon_3} &: \left(y(x); \alpha, \beta, \gamma, -\frac{1}{2} \right) \mapsto \left(\frac{\Phi - 2\varepsilon_1 xy}{\Phi}; \alpha', \beta', \gamma', -\frac{1}{2} \right), \end{aligned}$$

where $\varepsilon_1, \varepsilon_2, \varepsilon_3 \in \{-1, 1\}$ and

$$\begin{aligned} \alpha' &= \frac{1}{8} \left(\gamma + \varepsilon_1 \left(1 - \varepsilon_3 \sqrt{-2\beta} - \varepsilon_2 \sqrt{2\alpha} \right) \right)^2; \\ \beta' &= -\frac{1}{8} \left(\gamma - \varepsilon_1 \left(1 - \varepsilon_3 \sqrt{-2\beta} - \varepsilon_2 \sqrt{2\alpha} \right) \right)^2; \\ \gamma' &= \varepsilon_1 \left(\varepsilon_3 \sqrt{-2\beta} - \varepsilon_2 \sqrt{2\alpha} \right); \\ \Phi &= xy' - \varepsilon_2 \sqrt{2\alpha} y^2 + \varepsilon_3 \sqrt{-2\beta} + (\varepsilon_2 \sqrt{2\alpha} - \varepsilon_3 \sqrt{-2\beta} + \varepsilon_1 x)y. \end{aligned}$$

to so called seed solutions of P_V , which are given by

$$(3.3) \quad y = \begin{cases} \kappa x + \mu, & \text{for } \alpha = \frac{1}{2}, \beta = -\frac{1}{2}\mu^2, \gamma = \kappa(2 - \mu), \delta = -\frac{1}{2}\kappa^2; \\ \frac{\kappa}{x + \kappa}, & \text{for } \alpha = \frac{1}{2}, \beta = \kappa^2\mu, \gamma = 2\kappa\mu, \delta = \mu; \\ \frac{\kappa + x}{\kappa - x}, & \text{for } \alpha = \frac{1}{8}, \beta = -\frac{1}{8}, \gamma = -\kappa\mu, \delta = \mu, \end{cases}$$

where κ, μ are arbitrary constants.

In addition, P_V has the following elementary (non-rational) solutions:

$$(3.4) \quad \begin{aligned} y &= 1 + \kappa\sqrt{x}, & \text{for } \alpha = \mu, \beta = -\frac{1}{8}, \gamma = -\mu\kappa^2, \delta = 0; \\ y &= \kappa e^{\mu x}, & \text{for } \alpha = \beta = 0, \gamma = \mu, \delta = -\frac{1}{2}\mu^2, \end{aligned}$$

where κ, μ are arbitrary constants. For $\delta = 0$, algebraic solutions are all rational functions in \sqrt{x} and can be obtained by consecutive application of the Bäcklund transformations \mathcal{S}_1 and \mathcal{S}_2 to the first function of (3.4).

4. THE SOLUTIONS NEAR THE INFINITY SET

In this section, we study the behaviour of the solutions of the system (2.2) near the set \mathcal{I} , where the vector field is infinite. We prove that \mathcal{I} is a repeller for the solutions and that each solution which comes sufficiently close to \mathcal{I} at a certain point t will have a pole in a neighbourhood of t .

Lemma 4.1. *For every $\epsilon_1 > 0$ there exists a neighbourhood U of \mathcal{L}_2^p such that*

$$\left| \frac{E'}{E} + \theta_1 e^t \right| < \epsilon_1 \quad \text{in } U.$$

Proof. In the corresponding charts near \mathcal{L}_2^p (see Appendix A), the function

$$r = \frac{E'}{E} + \theta_1 e^t$$

is equal to:

$$r_{31} = \frac{\theta_1 e^t y_{31} z_{31} (\eta y_{31} - 2(\theta_0 y_{31} - 1)(y_{31} z_{31} - 1))}{\eta y_{31} (y_{31} z_{31} - 1) + F y_{31}^2 - \theta_0 y_{31} (y_{31} z_{31} - 1)^2 + y_{31}^2 z_{31}^2 - 2y_{31} z_{31} + 1},$$

$$r_{32} = \frac{\theta_1 e^t y_{32} z_{32} (\eta - 2(y_{32} - 1)(\theta_0 - z_{32}))}{(y_{32} - 1) z_{32} (\eta - (y_{32} - 1)(\theta_0 - z_{32})) + F}.$$

The statement of the lemma follows immediately from these expressions, since \mathcal{L}_2^p is given by $z_{31} = 0$ and $y_{32} = 0$. \square

Lemma 4.2. *For each compact subset K of $\mathcal{L}_1^p \setminus \mathcal{L}_8^p$ there exists a neighbourhood V of K and a constant $C > 0$ such that:*

$$\left| e^{-t} \frac{E'}{E} \right| < C \quad \text{in } V \text{ for all } t.$$

Proof. Near \mathcal{L}_1^p , in the respective coordinate charts (see Section A.2.2), we have:

$$e^{-t} \frac{E'}{E} \sim \begin{cases} -\frac{\theta_1 (y_{21} + 1)}{y_{21} - 1}, \\ \frac{\theta_1 (z_{22} + 1)}{z_{22} - 1}. \end{cases}$$

Since the projection of \mathcal{L}_8^p to these two charts is the point on \mathcal{L}_1^p given by coordinates $y_{21} = 1$ and $z_{22} = 0$, the statement is proved. \square

Lemma 4.3. *There exists a continuous complex valued function d on a neighbourhood of the infinity set \mathcal{I} in the Okamoto space, such that:*

$$d = \begin{cases} \frac{1}{E}, & \text{in a neighbourhood of } \mathcal{I} \setminus (\mathcal{L}_3^p \cup \mathcal{L}_4^p \cup \mathcal{L}_8^p \cup \mathcal{L}_9^p), \\ -J_{82}, & \text{in a neighbourhood of } \mathcal{L}_3^p \setminus \mathcal{L}_1^p, \\ -J_{102}, & \text{in a neighbourhood of } (\mathcal{L}_4^p \cup \mathcal{L}_8^p) \setminus \mathcal{L}_1^p, \\ -J_{112}, & \text{in a neighbourhood of } \mathcal{L}_9^p \setminus \mathcal{L}_8^p. \end{cases}$$

Proof. From Section A.2.8, the line \mathcal{L}_3^p is given by $z_{82} = 0$ in the (y_{82}, z_{82}) chart. Thus as we approach \mathcal{L}_3^p , i.e., as $z_{82} \rightarrow 0$, we have

$$E J_{82} \sim -1.$$

From Section A.2.10, the line \mathcal{L}_8^p is given by $z_{102} = 0$ in the (y_{102}, z_{102}) chart. Thus as we approach \mathcal{L}_8^p , i.e., as $z_{102} \rightarrow 0$, we have

$$E J_{102} \sim -1 - \frac{\theta_1 e^t}{y_{102}}.$$

In the same chart, the line \mathcal{L}_4^p is given by $y_{102} = -\theta_1 e^t$.

From Section A.2.11, the line \mathcal{L}_9^p is given by $z_{112} = 0$ in the (y_{112}, z_{112}) chart. We have:

$$\frac{J_{112}}{J_{102}} = 1 + \frac{(1 + \eta)\theta_1 e^t}{y_{112}}.$$

\square

Lemma 4.4 (Behaviour near $\mathcal{L}_3^p \setminus \mathcal{L}_1^p$). *If a solution at a complex time t is sufficiently close to $\mathcal{L}_3^p \setminus \mathcal{L}_1^p$, then there exists unique $\tau \in \mathbf{C}$ such that $(y(\tau), z(\tau))$ belongs to the line \mathcal{L}_7 . In other words, the solution has a pole at $t = \tau$.*

Moreover $|t - \tau| = O(|d(t)||y_{82}(t)|)$ for sufficiently small $d(t)$ and bounded $|y_{82}|$.

For large $R_3 > 0$, consider the set $\{t \in \mathbf{C} \mid |y_{82}| \leq R_3\}$. Its connected component containing τ is an approximate disk D_3 with centre τ and radius $|d(\tau)|R_3$, and $t \mapsto y_{82}(t)$ is a complex analytic diffeomorphism from that approximate disk onto $\{y \in \mathbf{C} \mid |y| \leq R_3\}$.

Proof. For the study of the solutions near $\mathcal{L}_3^p \setminus \mathcal{L}_1^p$, we use coordinates (y_{82}, z_{82}) . In this chart, the line $\mathcal{L}_3^p \setminus \mathcal{L}_1^p$ is given by the equation $z_{82} = 0$ and parametrised by $y_{82} \in \mathbf{C}$. Moreover, \mathcal{L}_7^p is given by $y_{82} = 0$ and parametrised by $z_{82} \in \mathbf{C}$.

Asymptotically, for $z_{82} \rightarrow 0$ and bounded y_{82}, e^{-t} , we have:

$$(4.1a) \quad y'_{82} \sim \frac{1}{z_{82}},$$

$$(4.1b) \quad z'_{82} \sim 4y_{82}^3 z_{82}^2,$$

$$(4.1c) \quad J_{82} = -z_{82},$$

$$(4.1d) \quad \frac{J'_{82}}{J_{82}} = \eta - 2\theta_0 - \theta_1 e^t - 4y_{82} + O(z_{82}) = \eta - 2\theta_0 - \theta_1 e^t - 4y_{82} + O(J_{82}),$$

$$(4.1e) \quad EJ_{82} \sim -1.$$

Integrating (4.1d) from τ to t , we get

$$J_{82}(t) = J_{82}(\tau) e^{K(t-\tau)} e^{-\theta_1(e^t - e^\tau)} (1 + o(1)),$$

$$K = \eta - 2\theta_0 - 4y_{82}(\tilde{\tau}),$$

where $\tilde{\tau}$ is on the integration path.

Because of (4.1b), z_{82} is approximately equal to a small constant, and from (4.1a) follows that:

$$y_{82} \sim y_{82}(\tau) + \frac{t - \tau}{z_{82}}.$$

Thus, if t runs over an approximate disk D centered at τ with radius $|z_{82}|R$, then y_{82} fills and approximate disk centered at $y_{82}(\tau)$ with radius R . Therefore, if $z_{82}(\tau) \ll \tau$, the solution has the following properties for $t \in D$:

$$\frac{z_{82}(t)}{z_{82}(\tau)} \sim 1,$$

and y_{82} is a complex analytic diffeomorphism from D onto an approximate disk with centre $y_{82}(\tau)$ and radius R . If R is sufficiently large, we will have $0 \in y_{82}(D)$, i.e. the solution of the Painlevé equation will have a pole at a unique point in D .

Now, it is possible to take τ to be the pole point. For $|t - \tau| \ll |\tau|$, we have:

$$\frac{d(t)}{d(\tau)} \sim 1, \quad \text{i.e.} \quad \frac{z_{82}(t)}{d(\tau)} \sim -\frac{J_{82}(t)}{d(\tau)} \sim 1,$$

$$y_{82}(t) \sim \frac{t - \tau}{z_{82}} \sim \frac{t - \tau}{d(\tau)}.$$

Let R_3 be a large positive real number. Then the equation $|y_{82}(t)| = R_3$ corresponds to $|t - \tau| \sim |d(\tau)|R_3$, which is still small compared to $|\tau|$ if $|d(\tau)|$ is sufficiently small. Denote by D_3 the connected component of the set of all $t \in \mathbf{C}$ such that $\{t \mid |y_{82}(t)| \leq R_3\}$ is an approximate disk with centre τ and radius $2|d(\tau)|R_3$. More precisely, y_{82} is a complex analytic diffeomorphism from D_3 onto $\{y \in \mathbf{C} \mid |y| \leq R_3\}$, and

$$\frac{d(t)}{d(\tau)} \sim 1 \quad \text{for all } t \in D_3.$$

We have $E(t)J_{82}(t) \sim -1$ when $|z_{82}| \ll 1$. Thus $E(t)J_{82}(t) \sim -1$ for the annular disk $t \in D_3 \setminus D'_3$, where D'_3 is a disk centered at τ with small radius compared to radius of D_3 . \square

Lemma 4.5 (Behaviour near $\mathcal{L}_9^p \setminus \mathcal{L}_8^p$). *If a solution at a complex time t is sufficiently close to $\mathcal{L}_9^p \setminus \mathcal{L}_8^p$, then there exists unique $\tau \in \mathbf{C}$ such that $(y(\tau), z(\tau))$ belongs to the line \mathcal{L}_{10} . In other words, the solution has a pole at $t = \tau$.*

Moreover $|t - \tau| = O(|d(t)||y_{112}(t)|)$ for sufficiently small $d(t)$ and bounded $|y_{112}|$.

For large $R_9 > 0$, consider the set $\{t \in \mathbf{C} \mid |y_{112}| \leq R_9\}$. Its connected component containing τ is an approximate disk D_9 with centre τ and radius $|d(\tau)|R_9$, and $\mapsto y_{112}(t)$ is a complex analytic diffeomorphism from that approximate disk onto $\{y \in \mathbf{C} \mid |y| \leq R_9\}$.

Proof. For the study of the solutions near $\mathcal{L}_9^p \setminus \mathcal{L}_8^p$, we use coordinates (y_{112}, z_{112}) . In this chart, the line $\mathcal{L}_9^p \setminus \mathcal{L}_8^p$ is given by the equation $z_{112} = 0$ and parametrised by $y_{112} \in \mathbf{C}$. Moreover, \mathcal{L}_{10}^p is given by $y_{112} = 0$ and parametrised by $z_{112} \in \mathbf{C}$.

Asymptotically, for $z_{112} \rightarrow 0$ and bounded y_{112} , e^{-t} , we have:

$$(4.2a) \quad y'_{112} \sim \frac{1}{z_{112}},$$

$$(4.2b) \quad z'_{112} \sim -3(1 + \eta)z_{112} - \frac{2}{\theta_1 e^t} y_{112} z_{112},$$

$$(4.2c) \quad J_{112} \sim -\theta_1 e^t z_{112},$$

$$(4.2d) \quad \frac{J'_{112}}{J_{112}} = -2 - \eta + \theta_1 e^t + O(z_{112}) = -2 - \eta + \theta_1 e^t + O(J_{112}),$$

$$(4.2e) \quad \frac{J_{112}}{J_{102}} = 1 + \frac{(1 + \eta)\theta_1 e^t}{y_{112}}.$$

Integrating (4.2d) from τ to t , we get

$$J_{112}(t) = J_{112}(\tau) e^{-(2+\eta)(t-\tau)} e^{\theta_1(e^t - e^\tau)} (1 + o(1)).$$

Because of (4.2c), z_{112} is approximately equal to a small constant, and from (4.2a) follows that:

$$y_{112} \sim y_{112}(\tau) + \frac{t - \tau}{z_{112}}.$$

Thus, if t runs over an approximate disk D centered at τ with radius $|z_{112}|R$, then y_{112} fills and approximate disk centered at $y_{112}(\tau)$ with radius R . Therefore, if $z_{112}(\tau) \ll \tau$, the solution has the following properties for $t \in D$:

$$\frac{z_{112}(t)}{z_{112}(\tau)} \sim 1,$$

and y_{112} is a complex analytic diffeomorphism from D onto an approximate disk with centre $y_{112}(\tau)$ and radius R . If R is sufficiently large, we will have $0 \in y_{112}(D)$, i.e. the solution of the Painlevé equation will have a pole at a unique point in D .

Now, it is possible to take τ to be the pole point. For $|t - \tau| \ll |\tau|$, we have:

$$\begin{aligned} \frac{d(t)}{d(\tau)} \sim 1, \quad \text{i.e.} \quad \frac{z_{112}(t)}{d(\tau)} \sim -\frac{1}{\theta_1 e^t} \cdot \frac{J_{112}(t)}{d(\tau)} \sim \frac{1}{\theta_1 e^t}, \\ y_{112}(t) \sim \frac{t - \tau}{z_{112}} \sim \frac{t - \tau}{d(\tau)} \cdot \theta_1 e^t. \end{aligned}$$

Let R_9 be a large positive real number. Then the equation $|y_{112}(t)| = R_9$ corresponds to $|(t - \tau)\theta_1 e^t| \sim |d(\tau)|R_9$, which is still small compared to $|\tau|$ if $|d(\tau)|$ is sufficiently small. Denote by D_9 the connected component of the set of all $t \in \mathbf{C}$ such that $\{t \mid |y_{112}(t)| \leq R_9\}$

is an approximate disk with centre τ and radius $2|d(\tau)|R_3$. More precisely, y_{112} is a complex analytic diffeomorphism from D_9 onto $\{y \in \mathbf{C} \mid |y| \leq R_9\}$, and

$$\frac{d(t)}{d(\tau)} \sim 1 \quad \text{for all } t \in D_9.$$

From (4.2e), we have:

$$\frac{J_{112}}{J_{102}} \sim 1 \quad \text{when } 1 \gg \left| \frac{(1+\eta)\theta_1 e^t}{y_{112}(t)} \right| \sim \left| \frac{(1+\eta)d(\tau)}{t-\tau} \right|,$$

that is, when

$$|t - \tau| \gg |d(\tau)|.$$

Since $R_9 \gg 1$, we have

$$|t - \tau| \sim |d(\tau)|R_9 \gg |d(\tau)|.$$

Thus $\frac{J_{112}}{J_{102}} \sim 1$ for the annular disk $t \in D_9 \setminus D'_9$, where D'_9 is a disk centered at τ with small radius compared to the radius of D_9 . \square

Lemma 4.6 (Behaviour near $\mathcal{L}_8^p \setminus \mathcal{L}_1^p$). *For large finite $R_8 > 0$, consider the set of all $t \in \mathbf{C}$, such that the solution at complex time t is close to $\mathcal{L}_8^p \setminus \mathcal{L}_1^p$, with $|y_{102}(t)| \leq R_8$, but not close to \mathcal{L}_9^p . Then this set is the complement of D_9 in an approximate disk D_8 with centre τ and radius $\sim \sqrt{|d(\tau)|}R_8$. More precisely, $t \mapsto y_{102}$ defines a covering from the annular domain $D_8 \setminus D_9$ onto the complement in $\{z \in \mathbf{C} \mid |z| \leq R_8\}$ of an approximate disk with centre at the origin and small radius $\sim |d(\tau)|R_9$, where $y_{102}(t) \sim d(\tau)^{-1/2}(t - \tau)$.*

Proof. Set $\mathcal{L}_8^p \setminus \mathcal{L}_1^p$ is visible in the chart (y_{102}, z_{102}) , where it is given by the equation $z_{102} = 0$ and parametrized by $y_{102} \in \mathbf{C}$, see Section A.2.10. In that chart, the line \mathcal{L}_9^p (without one point) is given by the equation $y_{102} = 0$ and parametrized by $z_{102} \in \mathbf{C}$. The line \mathcal{L}_4^p (without one point) is given by the equation $y_{102} = -\theta_1 e^t$ and also parametrized by $z_{102} \in \mathbf{C}$.

For $z_{102} \rightarrow 0$, bounded e^t , and y_{102} bounded and bounded away from $-\theta_1 e^t$, we have:

$$(4.3a) \quad z'_{102} \sim -\frac{1}{y_{102}} - \frac{1}{\theta_1 e^t + y_{102}} - \theta_1 e^t - 2y_{102},$$

$$(4.3b) \quad y'_{102} \sim \frac{2}{z_{102}},$$

$$(4.3c) \quad J_{102} = -y_{102}(\theta_1 e^t + y_{102})z_{102}^2,$$

$$(4.3d) \quad \frac{J'_{102}}{J_{102}} \sim \frac{(1+\eta)\theta_1 e^t}{y_{102}} + \theta_1 e^t + 2y_{102},$$

$$(4.3e) \quad EJ_{102} \sim 1 - \frac{\theta_1 e^t}{y_{102}}.$$

From (4.3d):

$$\begin{aligned} \log \frac{J_{102}(t_1)}{J_{102}(t_0)} &\sim \theta_1(e^{t_1} - e^{t_0}) + (t_1 - t_0)K, \\ K &= \frac{(1+\eta)\theta_1 e^{\tilde{\tau}}}{y_{102}(\tilde{\tau})} + 2y_{102}(\tilde{\tau}), \end{aligned}$$

where $\tilde{\tau}$ is on the integration path.

Therefore $J_{102}(t_1)/J_{102}(t_0) \sim 1$, if for all t on the segment from t_0 to t_1 we have $|t - t_0| \ll |t_0|$ and

$$\left| \frac{\theta_1 e^t}{y_{102}(t)} \right| \ll \frac{1}{|t_0|}, \quad |y_{102}(t)| \ll \frac{1}{|t_0|}.$$

We choose t_0 on the boundary of D_9 from Lemma 4.5. Then we have

$$\frac{d(\tau)}{d(t_0)} \sim \frac{J_{112}(\tau)}{J_{102}(t_0)} \sim 1 \quad \text{and} \quad |y_{112}(t_0)| = R_9,$$

which implies that

$$|z_{102}| = \left| \frac{1}{y_{112} + (1 + \eta)\theta_1 e^t} \right| \sim \frac{1}{R_9} \ll 1.$$

Since D_9 is an approximate disk with centre τ and small radius $\sim |d(\tau)|R_9$, and $R_9 \gg |\tau|^{-1}$, we have that $|y_{112}(t)| \geq R_9 \gg 1$ hence:

$$|y_{102}| \ll 1 \quad \text{if} \quad t = \tau + r(t_0 - \tau), \quad r \geq 1,$$

and

$$\frac{|t - t_0|}{|t_0|} = (r - 1) \left| 1 - \frac{\tau}{t_0} \right| \ll 1 \quad \text{if} \quad r - 1 \ll \frac{1}{\left| 1 - \frac{\tau}{t_0} \right|}.$$

Then equation (4.3c) and $J_{102} \sim -d(\tau)$ yield

$$z_{102}^{-1} \sim \left(\frac{y_{102}(\theta_1 e^t + y_{102})}{d(\tau)} \right)^{1/2} \sim \left(\frac{y_{102}^2}{d(\tau)} \right)^{1/2},$$

which in combination with (4.3a) leads to

$$\frac{dy_{102}}{dt} \sim d(\tau)^{-1/2}.$$

Hence

$$y_{102}(t) \sim y_{102}(t_0) + d(\tau)^{-1/2}(t - t_0),$$

and therefore

$$y_{102}(t) \sim d(\tau)^{-1/2}(t - t_0) \quad \text{if} \quad |t - t_0| \gg |y_{102}(t_0)|.$$

For large finite $R_8 > 0$, the equation $|y_{102}| = R_8$ corresponds to $|t - t_0| \sim \sqrt{d(\tau)}R_8$, which is still small compared to $|t_0| \sim |\tau|$, therefore $|t - \tau| \leq |t - t_0| + |t_0 - \tau| \leq |\tau|$. This proves the statement of the lemma. \square

Lemma 4.7 (Behaviour near \mathcal{L}_4^p). *For large finite $R_4 > 0$, consider the set of all $t \in \mathbf{C}$, such that the solution at complex time t is close to \mathcal{L}_4^p , with $|z_{91}(t)| \leq R_4$, but not close to \mathcal{L}_8^p . Then this set is the complement of D_8 in an approximate disk D_4 with centre τ and radius $\sim R_4/d(\tau)$. More precisely, $t \mapsto z_{91}$ defines a covering from the annular domain $D_4 \setminus D_8$ onto the complement in $\{z \in \mathbf{C} \mid |z| \leq R_4\}$ of an approximate disk with centre at the origin and small radius $\sim |d(\tau)|/R_8$, where $z_{91}(t) \sim d(\tau)/(t - \tau)$.*

Proof. \mathcal{L}_4^p without one point is visible in the chart (y_{91}, z_{91}) , where it is given by the equation $y_{91} = 0$ and parametrized by $z_{91} \in \mathbf{C}$, see Section A.2.9. In that chart, the line \mathcal{L}_1 is not visible, while \mathcal{L}_8 is given by the equation $z_{91} = 0$.

For $y_{91} \rightarrow 0$ and bounded z_{91} and e^t , we have:

$$(4.4a) \quad y'_{91} \sim -\frac{2\theta_1 e^t}{z_{91}},$$

$$(4.4b) \quad z'_{91} \sim \frac{\theta_1 e^t}{y_{91}},$$

$$(4.4c) \quad J_{102} = \frac{y_{91} z_{91}^2}{\theta_1 e^t - y_{91}},$$

$$(4.4d) \quad \frac{J'_{102}}{J_{102}} \sim -1 - \eta - \theta_1 e^t.$$

From (4.4d):

$$\log \frac{J_{102}(t_1)}{J_{102}(t_0)} \sim -(1 + \eta)(t_1 - t_0) - \theta_1(e^{t_1} - e^{t_0}).$$

Therefore $J_{102}(t_1)/J_{102}(t_0) \sim 1$ if for all t on the segment from t_0 to t_1 we have $|t - t_0| \ll t_0$. We choose t_0 on the boundary of D_8 from Lemma 4.6. Then we have

$$\frac{d(\tau)}{d(t_0)} \sim \frac{J_{102}(\tau)}{J_{102}(t_0)} \sim 1 \quad \text{and} \quad |y_{102}(t_0)| = R_8,$$

which implies that

$$|\theta_1 e^t| = |y_{91} - y_{102}| \sim R_8 \gg 1.$$

Hence:

$$|y_{91}| \ll 1 \quad \text{if} \quad |\theta_1 e^t| \sim R_8.$$

Then equation (4.4d) and $J_{102} \sim -d(\tau)$ yield

$$y_{91}^{-1} \sim -\frac{z_{91}^2}{\theta_1 e^t d(\tau)},$$

then, using (4.4b) we get:

$$\frac{d(z_{91}^{-1})}{dt} \sim \frac{1}{d(\tau)}.$$

It follows that

$$z_{91}^{-1} \sim z_{91}(t_0)^{-1} + \frac{t - t_0}{d(\tau)},$$

and therefore

$$z_{91} \sim \frac{d(\tau)}{t - t_0} \quad \text{if} \quad |t - t_0| \gg |z_{91}(t_0)^{-1}|.$$

For large finite $R_4 > 0$, the equation $|z_{91}| = R_4$ corresponds to $|t - t_0| \sim d(\tau)/R_4$, which is small compared to $|t_0| \sim |\tau|$, and therefore $|t - \tau| \leq |t - t_0| + |t_0 - \tau| \leq |\tau|$. This proves the statement of the lemma. \square

Theorem 4.8. *Let $\epsilon_1, \epsilon_2, \epsilon_3$ be given such that $\epsilon_1 > 0$, $0 < \epsilon_2 < |\theta_1|$, $0 < \epsilon_3 < 1$. Then there exists $\delta_1 > 0$ such that if $|e^{t_0}| < \epsilon_1$ and $|d(t_0)| < \delta_1$, then:*

$$\rho = \inf\{r < |e^{t_0}| \text{ such that } |d(t)| < \delta_1 \text{ whenever } |e^{t_0}| \geq |e^t| \geq r\}$$

satisfies:

- (i) $\delta_1 \geq |d(t_0)| (\rho |e^{t_0}|)^{\theta_1 - \epsilon_2} (1 - \epsilon_3)$;
- (ii) if $|e^{t_0}| \geq |e^t| \geq \rho$ then $d(t) = d(t_0) e^{\theta_1(t-t_0) + \epsilon_2 t} (1 + \epsilon_3(t))$;
- (iii) if $|e^t| \leq \rho$ then $d(t) \geq \delta_1 (1 - \epsilon_3)$.

Proof. Suppose a solution of the system (2.2) is close to the infinity set at times t_0 and t_1 . It follows from Lemmas 4.4–4.7 that for every solution close to \mathcal{I} , the set of complex time t such that the solution is not close to $\mathcal{L}_1^p \cup \mathcal{L}_2^p$ is the union of approximate disks of radius $\sim |d|$. Hence if the solution is near \mathcal{I} for all complex times t such that $|e^{t_0}| \geq |e^t| \geq |e^{t_1}|$, then there exists a path \mathcal{P} from t_0 to t_1 , such that the solution is close to $\mathcal{L}_1^p \cup \mathcal{L}_2^p$ for all $t \in \mathcal{P}$ and \mathcal{P} is C^1 -close to the path: $s \mapsto t_1^s t_0^{1-s}$, $s \in [0, 1]$.

Then Lemmas 4.1 and 4.2 imply that:

$$\log \frac{E(t)}{E(t_0)} = -\theta_1(t - t_0) \int_0^1 dt + o(1).$$

Therefore

$$E(t) = E(t_0) e^{-\theta_1(t-t_0) + o(1)} (1 + o(1)),$$

and

$$(4.5) \quad d(t) = d(t_0) e^{\theta_1(t-t_0) + o(1)} (1 + o(1)).$$

From Lemmas 4.4–4.7, we then have that, as long as the solution is close to \mathcal{I} , the ratio of d remains close to 1.

For the first statement of the theorem, we have:

$$\delta_1 > |d(t)| \geq |d(t_0)| |e^{\theta_1(t-t_0)-\epsilon_2}| (1 - \epsilon_3)$$

and so

$$\delta_1 \geq \sup_{\{t \mid |d(t)| < \delta_1\}} |d(t_0)| |e^{\theta_1(t-t_0)-\epsilon_2}| (1 - \epsilon_3).$$

The second statement follows from (4.5), while the third follows by the assumption on t . \square

5. THE LIMIT SET

In this section we consider properties of the limit set of the solutions, when $\operatorname{Re} t \rightarrow -\infty$, i.e. $x \rightarrow 0$.

Theorem 5.1. *There exists a compact subset K of $\mathcal{F}_\infty \setminus \mathcal{I}_\infty$, such that the limit set $\Omega_{(y,z)}$ of any solution (y, z) is contained in K . Moreover, $\Omega_{(y,z)}$ is a non-empty, compact and connected set, which is invariant under the flow of the autonomous system (2.5).*

Proof. For any positive numbers δ_1, r , let $K_{\delta_1, r}$ denote the set of all $s \in \mathcal{F}(t)$ such that $|e^t| \leq r$ and $d(s) \geq \delta_1$. Since $\mathcal{F}(t)$ is a complex analytic family over \mathbf{C} of compact surfaces, $K_{\delta_1, r}$ is also compact. Furthermore $K_{\delta_1, r}$ is disjoint from the union of the infinity sets $\mathcal{I}(t)$, $t \in \mathbf{C}$, and therefore $K_{\delta_1, r}$ is a compact subset of the Okamoto space $\mathcal{O} \setminus \mathcal{F}_0$. When r approaches zero, the sets $K_{\delta_1, r}$ shrink to the set

$$K_{\delta_1, 0} = \{s \in \mathcal{F}(0) \mid |d(s)| \geq \delta_1\} \subset \mathcal{F}_\infty \setminus \mathcal{I}_\infty,$$

which is compact.

It follows from Theorem 4.8 that there exists $\delta_1 \geq 0$ such that for every solution (y, z) there exists $r_0 > 0$ with the following property:

$$(y(t), z(t)) \in K_{\delta_1, r_0} \quad \text{for every } t \text{ such that } |e^t| \leq r_0.$$

In the sequel, we take $r \leq r_0$, when it follows that $(y(t), z(t)) \in K_{\delta_1, r}$ whenever $|e^t| \leq r$. Let $T_r = \{t \in \mathbf{C} \mid |e^t| \leq r\}$ and let $\Omega_{(y,z), r}$ denote the closure of $(y, z)(T_r)$ in \mathcal{O} . Since T_r is connected and (y, z) continuous, $\Omega_{(y,z), r}$ is also connected. Since $(y, z)(T_r)$ is contained in the compact subset $K_{\delta_1, r}$, its closure $\Omega_{(y,z), r}$ is also contained there and therefore $\Omega_{(y,z), r}$ is a non-empty compact and connected subset of $\mathcal{O} \setminus \mathcal{F}(0)$. The intersection of a decreasing sequence of non-empty compact and connected sets is non-empty, compact and connected: therefore, as $\Omega_{(y,z), r}$ decrease to $\Omega_{(y,z)}$ when r tends to zero, it follows that $\Omega_{(y,z)}$ is a non-empty, compact and connected set of \mathcal{O} . Since $\Omega_{(y,z), r} \subset K_{\delta_1, r}$ for all $r \leq r_0$, and the sets $K_{\delta_1, r}$ shrink to the compact subset $K_{\delta_1, 0}$ of $\mathcal{F}_\infty \setminus \mathcal{I}_\infty$ as r tends to zero, it follows that $\Omega_{(y,z)} \subset K_{\delta_1, 0}$. This proves the first statement of the theorem with $K = K_{\delta_1, 0}$.

Since $\Omega_{(y,z)}$ is the intersection of the decreasing family of compact sets $\Omega_{(y,z), r}$, there exists for every neighbourhood A of $\Omega_{(y,z)}$ in \mathcal{O} and $r > 0$ such that $\Omega_{(y,z), r} \subset A$, hence $(y(t), z(t)) \in A$ for every $t \in \mathbf{C}$ such that $|e^t| \leq r$. If t_j is any sequence in \mathbf{C} such that $\operatorname{Re} t_j \rightarrow -\infty$, then the compactness of $K_{\delta_1, r}$, in combination with $(y, z)T_r \subset K_{\delta_1, r}$, implies that there is a subsequence $j = j(k) \rightarrow \infty$ as $k \rightarrow \infty$, such that:

$$(y(t_{j(k)}), z(t_{j(k)})) \rightarrow s \quad \text{as } k \rightarrow \infty.$$

Then it follows that $s \in \Omega_{(y,z)}$.

Next we prove that $\Omega_{(y,z)}$ is invariant under the flow Φ^τ of the autonomous Hamiltonian system (2.5). Let $s \in \Omega_{(y,z)}$ and t_j be a sequence in \mathbf{C} such that $\operatorname{Re} t_j \rightarrow -\infty$ and $(y(t_j), z(t_j)) \rightarrow s$. Since the t -dependent vector field of the system (2.2) converges in C^1 to the vector field of the autonomous system (2.5) as $\operatorname{Re} t \rightarrow -\infty$, it follows from the continuous dependence on initial data and parameters, that the distance between $(y(t_j + \tau), z(t_j + \tau))$ and $\Phi^\tau(y(t_j), z(t_j))$

converges to zero as $j \rightarrow \infty$. Since $\Phi^\tau(y(t_j), z(t_j)) \rightarrow \Phi^\tau(s)$ and $\operatorname{Re} t_j \rightarrow -\infty$ as $j \rightarrow \infty$, it follows that $(y(t_j + \tau), z(t_j + \tau)) \rightarrow \Phi^\tau(s)$ and $t_j + t \rightarrow \infty$ as $j \rightarrow \infty$, hence $\Phi^\tau(s) \in \Omega_{(y,z)}$. \square

Proposition 5.2. *If y is a solution of (1.1) with essential singularity at $x = 0$, then the flow (y, z) of the vector field (2.2) meets each of the pole lines $\mathcal{L}_5, \mathcal{L}_6, \mathcal{L}_7$ infinitely many times.*

Proof. First, suppose that a solution $(y(t), z(t))$ intersects the union $\mathcal{L}_5 \cup \mathcal{L}_6 \cup \mathcal{L}_7$ only finitely many times.

According to Theorem 5.1, the limit set $\Omega_{(y,z)}$ is a compact set in $\mathcal{F}_\infty \setminus \mathcal{I}_\infty$. If $\Omega_{(y,z)}$ intersects one of the pole lines $\mathcal{L}_5, \mathcal{L}_6, \mathcal{L}_7$ at a point p , then there exists t with arbitrarily large negative real part such that $(u(t), v(t))$ is arbitrarily close to p , when the transversality of the vector field to the pole line implies that $(y(\tau), z(\tau)) \in \mathcal{L}_5 \cup \mathcal{L}_6 \cup \mathcal{L}_7$ for a unique τ near t . As this would imply that $(y(t), z(t))$ intersects $\mathcal{L}_5 \cup \mathcal{L}_6 \cup \mathcal{L}_7$ infinitely many times, it follows that $\Omega_{(y,z)}$ is a compact subset of $\mathcal{F}_\infty \setminus (\mathcal{I}_\infty \cup \mathcal{L}_5 \cup \mathcal{L}_6 \cup \mathcal{L}_7)$. It follows that $\Omega_{(y,z)}$ is a compact subset contained in the first affine chart, which implies that y and z remain bounded for large negative $\operatorname{Re} t$. Thus y, z are holomorphic functions of $x = e^t$ in a neighbourhood of $x = 0$, which implies that there are complex numbers $y(\infty), z(\infty)$ which are the limit points of $y(t), z(t)$ as $\operatorname{Re} t \rightarrow -\infty$. That means that y is analytic at $x = 0$, which contradicts the assumption that it has there an essential singularity.

Since the limit set $\Omega_{(y,z)}$ is invariant under the autonomous flow, it means that it will contain the whole irreducible component of a curve from the pencil $h_c(y, z) = 0$ given by (3.1), for some constant c . It is shown in Section 3.1 that this pencil of curves is birationally equivalent to a pencil of conics. We identified in Section 3.1 the three singular conics in the pencil and found the special solutions corresponding to them.

In all other cases, all three base points b_5, b_6, b_7 will be contained in the limit set, which are projections of the pole lines $\mathcal{L}_5(\infty), \mathcal{L}_6(\infty), \mathcal{L}_7(\infty)$ respectively. For a general solution (y, z) , the base point b_4 will not be contained in the limit set, because that point is not a base point of the autonomous system (2.4). \square

Remark 5.3. *If the limit set $\Omega_{(y,z)}$ contains only one point, that point must be a fixed point of the autonomous system (2.5). As we obtained in Section 2.2, there are four such points. One of the points has y -coordinate equal to unity and it corresponds to the rational solutions of the form $\frac{\kappa}{x + \kappa}$ and $\frac{\kappa + x}{\kappa - x}$.*

Theorem 5.4. *Every solution of (1.1) with essential singularity at $x = 0$ has infinitely many poles and infinitely many zeroes in each neighbourhood of that singular point.*

Proof. Applying results from Section 2.4 and Proposition 5.2, we get that each solution has a simple pole at the intersections with \mathcal{L}_5 and \mathcal{L}_6 and a simple zero at the intersection with \mathcal{L}_7 . \square

6. LIMIT $x \rightarrow \infty$

For studying the limit $x \rightarrow \infty$, it is convenient to represent the P_V as the following system:

$$(6.1) \quad \begin{aligned} y' &= \frac{1}{x} (2y(y-1)^2 z - (\theta_0 + \eta)y^2 + (2\theta_0 + \eta - \theta_1 x)y - \theta_0), \\ z' &= -\frac{1}{x} \left((y-1)(3y-1)z^2 - (2(\theta_0 + \eta)y - 2\theta_0 - \eta + \theta_1 x)z \right. \\ &\quad \left. + \frac{1}{2}\epsilon(\theta_0 + \eta - \theta_\infty) \right), \end{aligned}$$

where $\theta_\infty^2 = 2\alpha$, $\theta_0^2 = -2\beta$, $\theta_1^2 = -2\delta$ ($\theta_1 \neq 0$), $\eta = -\frac{\gamma}{\theta_1} - 1$, $\epsilon = \frac{1}{2}(\theta_0 + \theta_\infty + \eta)$.

Remark 6.1. Using the change of the independent variable $t = \log x$, equation (6.1) will give P_V in the form (2.1).

The resolution of the singularities of (6.1) will lead to the same space of the initial values as described in Section 2, and shown in Figure 3.

In the limit $x \rightarrow \infty$, the fifth Painlevé equation (1.1) becomes:

$$(6.2) \quad y'' = \left(\frac{1}{2y} + \frac{1}{y-1} \right) y'^2 + \frac{\delta y(y+1)}{y-1},$$

which has a first integral:

$$\frac{y'^2}{2y(y-1)} + \frac{\delta y}{(y-1)^2}.$$

The solutions of (6.2) are elliptic functions satisfying:

$$y'^2 = 2y(C(y-1)^2 - \delta y),$$

where C is an arbitrary constant. Notice that $y \equiv 0$ is the only solution of that equation taking the value 0. Thus, in contrast to the case when $x \rightarrow 0$, a_3 is not a base point for the autonomous equation, while a_4 will be a base point for that equation.

Now, analysing the system (6.1) in the similar way as shown in Sections 4 and 5, it follows in the limit $x \rightarrow \infty$, that a general solution of that system has a compact limit set which is invariant with the respect to the autonomous flow. This implies, as in the proof of Proposition 5.2, that the flow (y, z) of the vector field (6.1) meets each of the pole lines $\mathcal{L}_5, \mathcal{L}_6, \mathcal{L}_{10}$ infinitely many times. Thus every solution of (1.1) with essential singularity at $x = \infty$ has infinitely many poles and take the value 1 infinitely many times in each neighbourhood of that singular point.

APPENDIX A. RESOLUTION OF THE SYSTEM

A.1. The affine charts.

A.1.1. *Affine chart* (y_{01}, z_{01}) . The first affine chart is defined by the original coordinates: $y_{01} = y$, $z_{01} = z$. The energy (2.6) is:

$$E = y(y-1)^2 z^2 - (\theta_0 + \eta) y^2 z + (2\theta_0 + \eta) y z - \theta_0 z + \frac{1}{2} \epsilon (\theta_0 + \eta - \theta_\infty) y.$$

A.1.2. *Affine chart* (y_{02}, z_{02}) . The second affine chart is given by the coordinates:

$$\begin{aligned} y_{02} &= \frac{1}{y}, & z_{02} &= \frac{z}{y}, \\ y &= \frac{1}{y_{02}}, & z &= \frac{z_{02}}{y_{02}}. \end{aligned}$$

The line at infinity is $\mathcal{L}_\infty : y_{02} = 0$.

The Painlevé vector field (2.2) is:

$$\begin{aligned} y'_{02} &= -\frac{2z_{02}}{y_{02}^2} + \frac{4z_{02}}{y_{02}} + \eta + \theta_0 - (\eta + 2\theta_0)y_{02} + \theta_0 y_{02}^2 - 2z_{02} + \theta_1 e^t y_{02}, \\ z'_{02} &= -\frac{5z_{02}^2}{y_{02}^3} + \frac{8z_{02}^2}{y_{02}^2} + y_{02}(\theta_0 z_{02} - F) + \frac{3z_{02}(\eta + \theta_0 - z_{02})}{y_{02}} - 2(\eta + 2\theta_0)z_{02} + 2\theta_1 e^t z_{02}. \end{aligned}$$

In this chart, there is one visible base point:

$$a_0(y_{02} = 0, z_{02} = 0).$$

A.1.3. *Affine chart* (y_{03}, z_{03}) . The coordinates:

$$\begin{aligned} y_{03} &= \frac{y}{z}, & z_{03} &= \frac{1}{z}, \\ y &= \frac{y_{03}}{z_{03}}, & z &= \frac{1}{z_{03}}. \end{aligned}$$

The line at infinity is $\mathcal{L}_\infty : z_{03} = 0$.

The vector field (2.2) is:

$$\begin{aligned} y'_{03} &= \frac{5y_{03}^3}{z_{03}^3} - \frac{8y_{03}^2}{z_{03}^2} + \frac{3y_{03}(1 - (\eta + \theta_0)y_{03})}{z_{03}} + (Fy_{03} - \theta_0)z_{03} + 2(\eta + 2\theta_0)y_{03} - 2\theta_1 e^t y_{03}, \\ z'_{03} &= \frac{3y_{03}^2}{z_{03}^2} - \frac{4y_{03}}{z_{03}} + (\eta + 2\theta_0)z_{03} + Fz_{03}^2 + 1 - 2(\eta + \theta_0)y_{03} - \theta_1 e^t z_{03}. \end{aligned}$$

In this chart, there one base point:

$$a_1(y_{03} = 0, z_{03} = 0).$$

A.2. Blow ups.

A.2.1. Resolution at a_0 .

First chart:

$$\begin{aligned} y_{11} &= \frac{y_{02}}{z_{02}} = \frac{1}{z}, & z_{11} &= z_{02} = \frac{z}{y}, \\ y &= \frac{1}{y_{11}z_{11}}, & z &= \frac{1}{y_{11}}. \end{aligned}$$

The exceptional line is $\mathcal{L}_0 : z_{11} = 0$, while the proper preimage of the line at infinity \mathcal{L}_∞ is given by $y_{11} = 0$.

The vector field (2.2) in this chart is:

$$\begin{aligned} y'_{11} &= \frac{3}{y_{11}^2 z_{11}^2} - \frac{2(\eta + \theta_0)}{z_{11}} - \frac{4}{y_{11} z_{11}} + 1 + (\eta + 2\theta_0)y_{11} + Fy_{11}^2 - \theta_1 e^t y_{11}, \\ z'_{11} &= -\frac{5}{y_{11}^3 z_{11}} + \frac{8}{y_{11}^2} + \frac{3(\eta + \theta_0)}{y_{11}} - \frac{3z_{11}}{y_{11}} - 2(\eta + 2\theta_0)z_{11} - Fy_{11}z_{11} + \theta_0 y_{11} z_{11}^2 + 2\theta_1 e^t z_{11}. \end{aligned}$$

In this chart, there are no base points on the exceptional line \mathcal{L}_0 .

Second chart:

$$\begin{aligned} y_{12} &= y_{02} = \frac{1}{y}, & z_{12} &= \frac{z_{02}}{y_{02}} = z, \\ y &= \frac{1}{y_{12}}, & z &= z_{12}. \end{aligned}$$

The exceptional line is $\mathcal{L}_0 : y_{12} = 0$, while the proper preimage of the line at infinity \mathcal{L}_∞ is not visible in this chart.

The vector field (2.2) is:

$$\begin{aligned} y'_{12} &= -\frac{2z_{12}}{y_{12}} + \eta + \theta_0 - (\eta + 2\theta_0)y_{12} + \theta_0 y_{12}^2 + 4z_{12} - 2y_{12}z_{12} + \theta_1 e^t y_{12}, \\ z'_{12} &= -\frac{3z_{12}^2}{y_{12}^2} + \frac{4z_{12}^2}{y_{12}} + \frac{2(\eta + \theta_0)z_{12}}{y_{12}} - F - (\eta + 2\theta_0)z_{12} - z_{12}^2 + \theta_1 e^t z_{12}. \end{aligned}$$

In this chart, there is one base point on the exceptional line \mathcal{L}_0 :

$$a_2(y_{12} = 0, z_{12} = 0).$$

A.2.2. Resolution at a_1 .

First chart:

$$\begin{aligned} y_{21} &= \frac{y_{03}}{z_{03}} = y, & z_{21} &= z_{03} = \frac{1}{z}, \\ y &= y_{21}, & z &= \frac{1}{z_{21}}. \end{aligned}$$

The exceptional line is $\mathcal{L}_1 : z_{21} = 0$, while the proper preimage of the line at infinity \mathcal{L}_∞ is not visible in this chart.

The vector field (2.2) is:

$$\begin{aligned} y'_{21} &= \frac{2(y_{21} - 1)^2 y_{21}}{z_{21}} - \theta_0 + (\eta + 2\theta_0 - \theta_1 e^t) y_{21} - (\eta + \theta_0) y_{21}^2, \\ z'_{21} &= 1 - 4y_{21} + 3y_{21}^2 + (\eta + 2\theta_0 - \theta_1 e^t) z_{21} - 2(\eta + \theta_0) y_{21} z_{21} + F z_{21}^2. \end{aligned}$$

In this chart, there are two base points on the exceptional line \mathcal{L}_1 :

$$a_3(y_{21} = 0, z_{21} = 0), \quad a_4(y_{21} = 1, z_{21} = 0).$$

The energy (2.6) and its rate of change are:

$$\begin{aligned} E &= \frac{y_{21}(y_{21} - 1)^2}{z_{21}^2} - \frac{(y_{21} - 1)((\eta + \theta_0)y_{21} - \theta_0)}{z_{21}} + F y_{21}, \\ E' &= \theta_1 e^t \left(\frac{y_{21} - y_{21}^3}{z_{21}^2} + \frac{(\eta + \theta_0)y_{21}^2 - \theta_0}{z_{21}} - F y_{21} \right). \end{aligned}$$

Second chart:

$$\begin{aligned} y_{22} &= y_{03} = \frac{y}{z}, & z_{22} &= \frac{z_{03}}{y_{03}} = \frac{1}{y}, \\ y &= \frac{1}{z_{22}}, & z &= \frac{1}{y_{22} z_{22}}. \end{aligned}$$

The exceptional line is $\mathcal{L}_1 : y_{22} = 0$, while the proper preimage of the line at infinity \mathcal{L}_∞ is $z_{22} = 0$.

The vector field (2.2) is:

$$\begin{aligned} y'_{22} &= \frac{5}{z_{22}^3} - \frac{8}{z_{22}^2} + \frac{3(1 - (\eta + \theta_0)y_{22})}{z_{22}} - \theta_0 y_{22} z_{22} + F y_{22}^2 z_{22} + 2(\eta + 2\theta_0 - \theta_1 e^t) y_{22}, \\ z'_{22} &= -\frac{2(z_{22} - 1)^2}{y_{22} z_{22}^2} + \eta + \theta_0 - (\eta + 2\theta_0 - \theta_1 e^t) z_{22} + \theta_0 z_{22}^2. \end{aligned}$$

In this chart, the only visible base point on the exceptional line \mathcal{L}_1 is $(y_{22} = 0, z_{22} = 1)$, which is a_4 .

The energy (2.6) and its rate of change are:

$$\begin{aligned} E &= \frac{1}{y_{22}^2 z_{22}^5} - \frac{2}{y_{22}^2 z_{22}^4} + \frac{1}{y_{22}^2 z_{22}^3} - \frac{\eta + \theta_0}{y_{22} z_{22}^3} + \frac{\eta + 2\theta_0}{y_{22} z_{22}^2} - \frac{\theta_0}{y_{22} z_{22}} + \frac{F}{z_{22}}, \\ E' &= \frac{\theta_1 e^t}{y_{22}^2 z_{22}^5} \left(-F y_{22}^2 z_{22}^4 - \theta_0 y_{22} z_{22}^4 + (\eta + \theta_0) y_{22} z_{22}^2 + z_{22}^2 - 1 \right). \end{aligned}$$

A.2.3. Resolution at a_2 .

First chart:

$$y_{31} = \frac{y_{12}}{z_{12}} = \frac{1}{yz}, \quad z_{31} = z_{12} = z,$$

$$y = \frac{1}{y_{31}z_{31}}, \quad z = z_{31}.$$

The exceptional line is $\mathcal{L}_2 : z_{31} = 0$, while the proper preimage of the line \mathcal{L}_0 is $y_{31} = 0$.

The vector field (2.2) is:

$$y'_{31} = \frac{1 - (\eta + \theta_0)y_{31} + Fy_{31}^2}{y_{31}z_{31}} - y_{31}z_{31} + \theta_0y_{31}^2z_{31},$$

$$z'_{31} = -\frac{3}{y_{31}^2} + \frac{2(\eta + \theta_0)}{y_{31}} + \frac{4z_{31}}{y_{31}} - (\eta + 2\theta_0 - \theta_1e^t)z_{31} - z_{31}^2 - F.$$

There are two base points on the exceptional line \mathcal{L}_2 ; their y_{31} coordinates are the solutions of the quadratic equation:

$$1 - (\eta + \theta_0)y_{31} + Fy_{31}^2 = 0, \quad \text{where} \quad F = \frac{1}{4}(\theta_0 + \eta + \theta_\infty)(\theta_0 + \eta - \theta_\infty).$$

Thus, the base points are

$$a_5 \left(y_{31} = \frac{2}{\theta_0 + \eta + \theta_\infty}, z_{31} = 0 \right), \quad a_6 \left(y_{31} = \frac{2}{\theta_0 + \eta - \theta_\infty}, z_{31} = 0 \right).$$

The energy (2.6) and its rate of change are:

$$E = \frac{1}{y_{31}^3z_{31}} - \frac{\eta + \theta_0}{y_{31}^2z_{31}} - \frac{2}{y_{31}^2} + \frac{F}{y_{31}z_{31}} + \frac{2\theta_0 + \eta + z_{31}}{y_{31}} - \theta_0z_{31},$$

$$E' = -\theta_1e^t \left(\frac{1}{y_{31}^3z_{31}} - \frac{\eta + \theta_0}{y_{31}^2z_{31}} + \frac{F}{y_{31}z_{31}} - \frac{z_{31}}{y_{31}} + \theta_0z_{31} \right).$$

Second chart:

$$y_{32} = y_{12} = \frac{1}{y}, \quad z_{32} = \frac{z_{12}}{y_{12}} = yz,$$

$$y = \frac{1}{y_{32}}, \quad z = y_{32}z_{32}.$$

The exceptional line is $\mathcal{L}_2 : y_{32} = 0$, while the proper preimage of the line \mathcal{L}_0 is not visible in this chart.

The vector field (2.2) is:

$$y'_{32} = \eta + \theta_0 - (\eta + 2\theta_0 - \theta_1e^t)y_{32} + \theta_0y_{32}^2 - 2z_{32} + 4y_{32}z_{32} - 2y_{32}^2z_{32},$$

$$z'_{32} = -\frac{F - (\eta + \theta_0)z_{32} + z_{32}^2}{y_{32}} - \theta_0y_{32}z_{32} + y_{32}z_{32}^2.$$

In this chart, the only base points on the exceptional line \mathcal{L}_2 are a_5 and a_6 .

The energy (2.6) and its rate of change are:

$$E = \frac{F - (\eta + \theta_0)z_{32} + z_{32}^2}{y_{32}} + (\eta + 2\theta_0)z_{32} - \theta_0y_{32}z_{32} + y_{32}z_{32}^2 - 2z_{32}^2,$$

$$E' = -\theta_1e^t \left(\frac{F - (\eta + \theta_0)z_{32} + z_{32}^2}{y_{32}} + \theta_0y_{32}z_{32} - y_{32}z_{32}^2 \right).$$

A.2.4. Resolution at a_3 .

First chart:

$$y_{41} = \frac{y_{21}}{z_{21}} = yz, \quad z_{41} = z_{21} = \frac{1}{z},$$

$$y = y_{41}z_{41}, \quad z = \frac{1}{z_{41}}.$$

The exceptional line is $\mathcal{L}_3 : z_{41} = 0$, while the proper preimage of the line \mathcal{L}_1 is not visible in this chart.

The vector field (2.2) is:

$$y'_{41} = \frac{y_{41} - \theta_0}{z_{41}} - Fy_{41}z_{41} + \eta y_{41}^2 z_{41} + \theta_0 y_{41}^2 z_{41} - y_{41}^3 z_{41},$$

$$z'_{41} = 1 + (\eta + 2\theta_0 - \theta_1 e^t)z_{41} - 4y_{41}z_{41} + Fz_{41}^2 - 2\eta y_{41}z_{41}^2 - 2\theta_0 y_{41}z_{41}^2 + 3y_{41}^2 z_{41}^2.$$

In this chart, there is one base point on the exceptional line \mathcal{L}_3 :

$$a_7(y_{41} = \theta_0, z_{41} = 0).$$

The energy (2.6) is:

$$E = \frac{y_{41} - \theta_0}{z_{41}} + y_{41}^3 z_{41} - (\eta + \theta_0)y_{41}^2 z_{41} - 2y_{41}^2 + Fy_{41}z_{41} + (2\theta_0 + \eta)y_{41}.$$

Second chart:

$$y_{42} = y_{21} = y, \quad z_{42} = \frac{z_{21}}{y_{21}} = \frac{1}{yz},$$

$$y = y_{42}, \quad z = \frac{1}{y_{42}z_{42}}.$$

The exceptional line is $\mathcal{L}_3 : y_{42} = 0$, while the proper preimage of the line \mathcal{L}_1 is $z_{42} = 0$.

The vector field (2.2) is:

$$y'_{42} = \frac{2(y_{42} - 1)^2}{z_{42}} - \theta_0 + (\eta + 2\theta_0 - \theta_1 e^t)y_{42} - (\eta + \theta_0)y_{42}^2,$$

$$z'_{42} = \frac{\theta_0 z_{42} - 1}{y_{42}} + y_{42} - (\eta + \theta_0)y_{42}z_{42} + Fy_{42}z_{42}^2.$$

In this chart, the only base point on the exceptional line \mathcal{L}_3 is $a_7(y_{42} = 0, z_{42} = 1/\theta_0)$.

The energy (2.6) is:

$$E = \frac{1}{y_{42}z_{42}^2} + \frac{y_{42} - 2}{z_{42}^2} - \frac{\theta_0}{y_{42}z_{42}} + \frac{2\theta_0 + \eta - (\theta_0 + \eta)y_{42}}{z_{42}} + Fy_{42}.$$

A.2.5. Resolution at a_4 .

First chart:

$$y_{51} = \frac{y_{21} - 1}{z_{21}} = (y - 1)z, \quad z_{51} = z_{21} = \frac{1}{z},$$

$$y = y_{51}z_{51} + 1, \quad z = \frac{1}{z_{51}}.$$

The exceptional line is $\mathcal{L}_4 : z_{51} = 0$, while the proper preimage of the line \mathcal{L}_1 is not visible in this chart.

The vector field (2.2) is:

$$y'_{51} = -\frac{\theta_1 e^t}{z_{51}} - Fy_{51}z_{51} + (\eta + \theta_0)y_{51}^2 z_{51} - y_{51}^3 z_{51},$$

$$z'_{51} = -(\eta + \theta_1 e^t)z_{51} + 2y_{51}z_{51} + Fz_{51}^2 - 2(\eta + \theta_0)y_{51}z_{51}^2 + 3y_{51}^2 z_{51}^2.$$

There are no base points on the exceptional line \mathcal{L}_4 in this chart.

The energy (2.6) is:

$$E = y_{51}^3 z_{51} - (\eta + \theta_0) y_{51}^2 z_{51} + y_{51}^2 + F y_{51} z_{51} - \eta y_{51} + F.$$

Second chart:

$$y_{52} = y_{21} - 1 = y - 1, \quad z_{52} = \frac{z_{21}}{y_{21} - 1} = \frac{1}{(y - 1)z},$$

$$y = y_{52} + 1, \quad z = \frac{1}{y_{52} z_{52}}.$$

The exceptional line is $\mathcal{L}_4 : y_{52} = 0$, while the proper preimage of the line \mathcal{L}_1 is $z_{52} = 0$.

The vector field (2.2) is:

$$y'_{52} = -\theta_0 + (\eta + 2\theta_0 - \theta_1 e^t)(1 + y_{52}) - (\eta + \theta_0)(1 + y_{52})^2 + \frac{2y_{52}(1 + y_{52})}{z_{52}},$$

$$z'_{52} = \frac{\theta_1 e^t z_{52}}{y_{52}} + y_{52} - (\eta + \theta_0) y_{52} z_{52} + F y_{52} z_{52}^2.$$

In this chart, there is one base point on the exceptional line \mathcal{L}_4 :

$$a_8(y_{52} = 0, z_{52} = 0).$$

Notice that a_8 is the intersection point of \mathcal{L}_4 and the proper preimage of \mathcal{L}_1 .

The energy (2.6) is:

$$E = \frac{y_{52} + 1}{z_{52}^2} - \frac{(\eta + \theta_0)y_{52} + \eta}{z_{52}} + F y_{52} + F.$$

A.2.6. Resolution at a_5 .

First chart:

$$\tilde{y}_{61} = \frac{y_{32}}{z_{32} - \epsilon} = \frac{1}{y(yz - \epsilon)}, \quad \tilde{z}_{61} = z_{32} - \epsilon = yz - \epsilon,$$

$$y = \frac{1}{\tilde{y}_{61} \tilde{z}_{61}}, \quad z = \tilde{y}_{61} \tilde{z}_{61} (\tilde{z}_{61} + \epsilon).$$

The exceptional line is $\mathcal{L}_5 : z_{61} = 0$, and the proper preimage of \mathcal{L}_2 is $y_{61} = 0$. \mathcal{L}_0 is not visible in this chart.

The vector field (2.2) is:

$$y'_{61} = -1 + (4\epsilon - \eta - 2\theta_0 + \theta_1 e^t) y_{61} + \epsilon(\epsilon - \theta_0) y_{61}^2 + 4y_{61} z_{61} + 2(\theta_0 - 2\epsilon) y_{61}^2 z_{61} - 3y_{61}^2 z_{61}^2,$$

$$z'_{61} = \frac{\eta + \theta_0 - 2\epsilon - z_{61}}{y_{61}} + \epsilon(\epsilon - \theta_0) y_{61} z_{61} + (2\epsilon - \theta_0) y_{61} z_{61}^2 + y_{61} z_{61}^3.$$

In this chart, there are no base points on the exceptional line \mathcal{L}_5 .

The energy (2.6) is:

$$E = \frac{2\epsilon - \eta - \theta_0 + z_{61}}{y_{61}} + \epsilon(\eta + 2\theta_0 - 2\epsilon) + (\eta - 4\epsilon + 2\theta_0) z_{61} - 2z_{61}^2$$

$$+ \epsilon(\epsilon - \theta_0) y_{61} z_{61} + (2\epsilon - \theta_0) y_{61} z_{61}^2 + y_{61} z_{61}^3.$$

Second chart:

$$\tilde{y}_{62} = y_{32} = \frac{1}{y}, \quad \tilde{z}_{62} = \frac{z_{32} - \epsilon}{y_{32}} = y(yz - \epsilon),$$

$$y = \frac{1}{\tilde{y}_{62}}, \quad z = \tilde{y}_{62} (y_{62} \tilde{z}_{62} + \epsilon).$$

The exceptional line is $\mathcal{L}_5 : y_{62} = 0$, while the proper preimages of \mathcal{L}_2 and \mathcal{L}_0 are not visible in this chart.

The vector field (2.2) is:

$$\begin{aligned} y'_{62} &= \eta - 2\epsilon + \theta_0 + (4\epsilon - \eta - 2\theta_0 + \theta_1 e^t)y_{62} + (\theta_0 - 2\epsilon)y_{62}^2 - 2y_{62}z_{62} + 4y_{62}^2z_{62} - 2y_{62}^3z_{62}, \\ z'_{62} &= \epsilon(\epsilon - \theta_0) + (\eta + 2\theta_0 - 4\epsilon - \theta_1 e^t)z_{62} + z_{62}^2 + 2(2\epsilon - \theta_0)y_{62}z_{62} - 4y_{62}z_{62}^2 + 3y_{62}^2z_{62}^2. \end{aligned}$$

In this chart, there are no base points on the exceptional line \mathcal{L}_5 .

The energy (2.6) is:

$$\begin{aligned} E &= \epsilon(\eta - 2\epsilon + 2\theta_0) + \epsilon(\epsilon - \theta_0)y_{62} + (2\epsilon - \eta - \theta_0)z_{62} \\ &\quad + (\eta - 4\epsilon + 2\theta_0)y_{62}z_{62} + (2\epsilon - \theta_0)y_{62}^2z_{62} + y_{62}z_{62}^2 - 2y_{62}^2z_{62}^2 + y_{62}^3z_{62}^2. \end{aligned}$$

A.2.7. *Resolution at a_6 .* Same as at a_5 , replacing θ_∞ with $-\theta_\infty$. The resolution does not yield new base points.

A.2.8. *Resolution at a_7 .*

First chart:

$$\begin{aligned} y_{81} &= \frac{y_{41} - \theta_0}{z_{41}} = z(yz - \theta_0), \quad z_{81} = z_{41} = \frac{1}{z}, \\ y &= z_{81}(y_{81}z_{81} + \theta_0), \quad z = \frac{1}{z_{81}}. \end{aligned}$$

The exceptional line is $\mathcal{L}_7 : z_{81} = 0$, while the proper preimages of the lines \mathcal{L}_3 and \mathcal{L}_1 are not visible in this chart.

The vector field (2.2) is:

$$\begin{aligned} y'_{81} &= \theta_0(\eta\theta_0 - F) + (2\theta_0 - \eta + \theta_0 e^t)y_{81} + 2(2\eta\theta_0 - \theta_0^2 - F)y_{81}z_{81} \\ &\quad + 4y_{81}^2z_{81} + 3(\eta - 2\theta_0)y_{81}^2z_{81}^2 - 4y_{81}^3z_{81}^3, \\ z'_{81} &= 1 + (\eta - 2\theta_0 - \theta_1 e^t)z_{81} + (F - 2\eta\theta_0 + \theta_0^2)z_{81}^2 - 4y_{81}z_{81}^2 + 2(2\theta_0 - \eta)y_{81}z_{81}^3 + 3y_{81}^2z_{81}^4. \end{aligned}$$

There are no base points on \mathcal{L}_7 in this chart.

The energy (2.6) is:

$$\begin{aligned} E &= \eta\theta_0 + y_{81} + \theta_0(F - \eta\theta_0)z_{81} + (\eta - 2\theta_0)y_{81}z_{81} \\ &\quad + (F + \theta_0^2 - 2\eta\theta_0)y_{81}z_{81}^2 - 2y_{81}^2z_{81}^2 + (2\theta_0 - \eta)y_{81}^2z_{81}^3 + y_{81}^3z_{81}^4. \end{aligned}$$

Second chart:

$$\begin{aligned} y_{82} &= y_{41} - \theta_0 = yz - \theta_0, \quad z_{82} = \frac{z_{41}}{y_{41} - \theta_0} = \frac{1}{z(yz - \theta_0)}, \\ y &= y_{82}z_{82}(y_{82} + \theta_0), \quad z = \frac{1}{y_{82}z_{82}}. \end{aligned}$$

The Jacobian and its derivative are:

$$\begin{aligned} J_{82} &= \frac{\partial y_{82}}{\partial y} \frac{\partial z_{82}}{\partial z} - \frac{\partial y_{82}}{\partial z} \frac{\partial z_{82}}{\partial y} = \frac{1}{z(\theta_0 - yz)} = -z_{82}, \\ J'_{82} &= -z_{82}(\eta - 2\theta_0 - \theta_1 e^t - 4y_{82} + \theta_0(F - \eta\theta_0)z_{82} + 2(F - 2\eta\theta_0 + \theta_0^2)y_{82}z_{82} \\ &\quad + 3(2\theta_0 - \eta)y_{82}^2z_{82} + 4y_{82}^3z_{82}). \end{aligned}$$

The exceptional line is $\mathcal{L}_7 : y_{82} = 0$, while the proper preimage of the line \mathcal{L}_3 is $z_{82} = 0$. \mathcal{L}_1 is not visible in this chart.

The vector field (2.2) is:

$$\begin{aligned} y'_{82} &= \frac{1}{z_{82}} + \theta_0(\eta\theta_0 - F)y_{82}z_{82} + (2\eta\theta_0 - \theta_0^2 - F)y_{82}^2z_{82} + (\eta - 2\theta_0)y_{82}^3z_{82} - y_{82}^4z_{82}, \\ z'_{82} &= z_{82}(\eta - 2\theta_0 - \theta_1 e^t - 4y_{82} + \theta_0(F - \eta\theta_0)z_{82} + 2(F - 2\eta\theta_0 + \theta_0^2)y_{82}z_{82} \\ &\quad + 3(2\theta_0 - \eta)y_{82}^2z_{82} + 4y_{82}^3z_{82}). \end{aligned}$$

In this chart, no base points are visible on the exceptional line \mathcal{L}_7 .

The energy (2.6) is:

$$E = \frac{1}{z_{82}} + \eta\theta_0 + (\eta - 2\theta_0)y_{82} - 2y_{82}^2 + \theta_0(F - \eta\theta_0)y_{82}z_{82} \\ + (F - 2\eta\theta_0 + \theta_0^2)y_{82}^2z_{82} + (2\theta_0 - \eta)y_{82}^3z_{82} + y_{82}^4z_{82}.$$

A.2.9. *Resolution at a_8 .*

First chart:

$$y_{91} = \frac{y_{52}}{z_{52}} = (y - 1)^2z, \quad z_{91} = z_{52} = \frac{1}{(y - 1)z}, \\ y = y_{91}z_{91} + 1, \quad z = \frac{1}{y_{91}z_{91}^2}.$$

The exceptional line is $\mathcal{L}_8 : z_{91} = 0$, while the proper preimage of the line \mathcal{L}_4 is $y_{91} = 0$. \mathcal{L}_1 is not visible in this chart and it corresponds to the infinite value of y_{91} .

The vector field (2.2) is:

$$y'_{91} = \frac{2(y_{91} - \theta_1 e^t)}{z_{91}} - (\eta + \theta_1 e^t)y_{91} + y_{91}^2 - Fy_{91}^2z_{91}^2, \\ z'_{91} = \frac{\theta_1 e^t}{y_{91}} + y_{91}z_{91}(1 - (\eta + \theta_0)z_{91} + Fz_{91}^2).$$

In this chart, there is one base point on the exceptional line \mathcal{L}_8 :

$$a_9(y_{91} = \theta_1 e^t, z_{91} = 0).$$

The energy (2.6) is:

$$E = \frac{1}{z_{91}^2} + \frac{y_{91} - \eta}{z_{91}} + F - (\eta + \theta_0)y_{91} + Fy_{91}z_{91}.$$

Second chart:

$$y_{92} = y_{52} = y - 1, \quad z_{92} = \frac{z_{52}}{y_{52}} = \frac{1}{(y - 1)^2z}, \\ y = y_{92} + 1, \quad z = \frac{1}{y_{92}^2z_{92}}.$$

The exceptional line is $\mathcal{L}_8 : y_{92} = 0$. The proper preimage of the line \mathcal{L}_1 is $z_{92} = 0$, while the proper preimage of \mathcal{L}_4 is not visible in this chart.

The vector field (2.2) is:

$$y'_{92} = \frac{2(1 + y_{92})}{z_{92}} - \theta_1 e^t - (\eta + \theta_1 e^t)y_{92} - (\eta + \theta_0)y_{92}^2, \\ z'_{92} = \frac{2(\theta_1 e^t z_{92} - 1)}{y_{92}} + (\eta + \theta_1 e^t)z_{92} + Fy_{92}^2z_{92}^2 - 1.$$

In this chart, there is one base point on the exceptional line \mathcal{L}_8 : $a_9 \left(y_{92} = 0, z_{92} = \frac{1}{\theta_1 e^t} \right)$.

The energy (2.6) is:

$$E = \frac{1}{y_{92}^2z_{92}^2} + \frac{1}{y_{92}z_{92}^2} - \frac{\eta}{y_{92}z_{92}} - \frac{\eta + \theta_0}{z_{92}} + Fy_{92} + F.$$

A.2.10. *Resolution at a_9 .*

First chart:

$$y_{101} = \frac{y_{91} - \theta_1 e^t}{z_{91}} = (y-1)z((y-1)^2z - \theta_1 e^t), \quad z_{101} = z_{91} = \frac{1}{(y-1)z},$$

$$y = 1 + \theta_1 e^t z_{101} + y_{101} z_{101}^2, \quad z = \frac{1}{z_{101}^2(\theta_1 e^t + y_{101} z_{101})}.$$

The exceptional line is $\mathcal{L}_9 : z_{101} = 0$, while the proper preimage of \mathcal{L}_8 is not visible in this chart.

The vector field (2.2) is:

$$y'_{101} = \frac{\theta_1 e^t (y_{101} - (1+\eta)\theta_1 e^t)}{z_{101}(\theta_1 e^t + y_{101} z_{101})} + \frac{y_{101}(2y_{101} - (1+\eta)\theta_1 e^t)}{\theta_1 e^t + y_{101} z_{101}} - \eta y_{101} - F\theta_1^2 e^{2t} z_{101}$$

$$+ \theta_1(\eta + \theta_0) e^t y_{101} z_{101} - 3F\theta_1 e^t y_{101} z_{101}^2 + (\eta + \theta_0) y_{101}^2 z_{101}^2 - 2F y_{101}^2 z_{101}^3,$$

$$z'_{101} = \frac{\theta_1 e^t}{\theta_1 e^t + y_{101} z_{101}} + \theta_1 e^t z_{101} - (\eta + \theta_0) \theta_1 e^t z_{101}^2 + y_{101} z_{101}^2 + F\theta_1 e^t z_{101}^3$$

$$- (\eta + \theta_0) y_{101} z_{101}^3 + F y_{101} z_{101}^4.$$

In this chart, there one base point on the exceptional line \mathcal{L}_9 :

$$a_{10} (y_{101} = (1+\eta)\theta_1 e^t, z_{101} = 0).$$

The energy (2.6):

$$E = \frac{1}{z_{101}^2} + \frac{\theta_1 e^t - \eta}{z_{101}} - (\eta + \theta_0) \theta_1 e^t + F + y_{101} + \theta_1 e^t F z_{101} - (\eta + \theta_0) y_{101} z_{101} + F y_{101} z_{101}^2.$$

Second chart:

$$y_{102} = y_{91} - \theta_1 e^t = (y-1)^2 z - \theta_1 e^t, \quad z_{102} = \frac{z_{91}}{y_{91} - \theta_1 e^t} = \frac{1}{(y-1)z} \cdot \frac{1}{(y-1)^2 z - \theta_1 e^t},$$

$$y = 1 + \theta_1 e^t y_{102} z_{102} + y_{102}^2 z_{102}, \quad z = \frac{1}{y_{102}^2(\theta_1 e^t + y_{102}) z_{102}^2}.$$

The Jacobian is:

$$J_{102} = \frac{\partial y_{102}}{\partial y} \frac{\partial z_{102}}{\partial z} - \frac{\partial y_{102}}{\partial z} \frac{\partial z_{102}}{\partial y} = \frac{1}{z(\theta_1 e^t - (y-1)^2 z)} = -y_{102}(\theta_1 e^t + y_{102}) z_{102}^2,$$

$$J'_{102} = -2y_{102}^3 z_{102}^2 (1 - (\eta + \theta_0) y_{102} z_{102} + F y_{102}^2 z_{102}^2) - F\theta_1^3 e^{3t} y_{102}^2 z_{102}^4$$

$$- \theta_1^2 e^{2t} z_{102}^2 (1 + \eta + y_{102} - 2(\eta + \theta_0) y_{102}^2 z_{102} + 4F y_{102}^3 z_{102}^2)$$

$$- \theta_1 e^t y_{102} z_{102}^2 (1 + \eta + 3y_{102} - 4(\eta + \theta_0) y_{102}^2 z_{102} + 5F y_{102}^3 z_{102}^2).$$

The exceptional line is $\mathcal{L}_9 : y_{102} = 0$. The proper preimages of \mathcal{L}_8 is $z_{102} = 0$ and of \mathcal{L}_4 is $y_{102} = -\theta_1 e^t$. \mathcal{L}_1 is not visible in this chart and it corresponds the infinite value of y_{102} .

The vector field (2.2) is:

$$y'_{102} = \frac{2}{z_{102}} - \eta y_{102} + y_{102}^2 - F y_{102}^4 z_{102}^2 - (1+\eta)\theta_1 e^t$$

$$+ \theta_1 e^t y_{102} - F\theta_1^2 e^{2t} y_{102}^2 z_{102}^2 - 2F\theta_1 e^t y_{102}^3 z_{102}^2,$$

$$z'_{102} = \frac{\theta_1 e^t((1+\eta)\theta_1 e^t z_{102} - 1)}{y_{102}(\theta_1 e^t + y_{102})} + \frac{(1+\eta)\theta_1 e^t z_{102} - 2}{\theta_1 e^t + y_{102}}$$

$$- \theta_1 e^t + (1+\eta)\theta_1^2 e^{2t} z_{102} - 2y_{102} + (1+\eta)\theta_1 e^t y_{102} z_{102}.$$

In this chart, there is one visible base point on the exceptional line $\mathcal{L}_9 : a_{10} \left(y_{102} = 0, z_{102} = \frac{1}{(1+\eta)\theta_1 e^t} \right)$.

The energy (2.6) is:

$$E = \frac{1}{y_{102}^2 z_{102}^2} + \frac{\theta_1 e^t - \eta}{y_{102} z_{102}} + \frac{1}{z_{102}} + F - (\eta + \theta_0) \theta_1 e^t - (\eta + \theta_0) y_{102} + e^t F \theta_1 y_{102} z_{102} + F y_{102}^2 z_{102}.$$

A.2.11. *Resolution at a_{10} .*

First chart:

$$\begin{aligned} y_{111} &= \frac{y_{101} - (1 + \eta)\theta_1 e^t}{z_{101}} = (y - 1)^4 z^3 - \theta_1 e^t (y - 1)^2 z^2 - (1 + \eta)\theta_1 e^t (y - 1)z, \\ z_{111} &= z_{101} = \frac{1}{(y - 1)z}, \\ y &= 1 + \theta_1 e^t z_{111} + \theta_1 e^t z_{111}^2 + \eta \theta_1 e^t z_{111}^2 + y_{111} z_{111}^3, \\ z &= \frac{1}{z_{111}^2 (\theta_1 e^t + \theta_1 e^t z_{111} + \eta \theta_1 e^t z_{111} + y_{111} z_{111}^2)}. \end{aligned}$$

The exceptional line is $\mathcal{L}_{10} : z_{111} = 0$, while the proper preimage of \mathcal{L}_9 is not visible in this chart.

The vector field (2.2) is:

$$\begin{aligned} y'_{111} &= \frac{1}{y_{111} z_{111}^2 + \theta_1 e^t (1 + (1 + \eta)z_{111})} \times \\ &\quad \times \left((e^{3t} \theta_1^3 (1 + (1 + \eta)z_{111})^2 (\eta^2 + \theta_0 - F(1 + 2z_{111}) + \eta(1 + \theta_0 - 2Fz_{111}))) \right. \\ &\quad - y_{111}^2 z_{111} (y_{111} z_{111}^3 (1 - 2\theta_0 z_{111} + 3Fz_{111}^2) + \eta(z_{111} - 2y_{111} z_{111}^4) - 2) \\ &\quad + \theta_1 e^t y_{111} (3 - z_{111} - 2y_{111} z_{111}^2 + 2(2\theta_0 - 1)y_{111} z_{111}^3 + (5\theta_0 y_{111} - 7Fy_{111})z_{111}^4) \\ &\quad + \theta_1 e^t y_{111} (\eta^2 z_{111} (5y_{111} z_{111}^3 - 2) - 8Fy_{111} z_{111}^5) \\ &\quad + \eta \theta_1 e^t y_{111} (2 - 3z_{111} + 2y_{111} z_{111}^3 + 5(1 + \theta_0)y_{111} z_{111}^4 - 8Fy_{111} z_{111}^5) \\ &\quad - e^{2t} \theta_1^2 (1 + y_{111}(1 + z_{111}))(1 + z_{111} - 2\theta_0 z_{111} + (5F - 4\theta_0)z_{111}^2 + 7Fz_{111}^3) \\ &\quad + \eta \theta_1^2 e^{2t} (2y_{111} z_{111}^2 (2 + 3\theta_0 + 2(1 - 3F + 2\theta_0 + 2\eta^2)z_{111} - 7Fz_{111}^2) - 3 - \eta^2) \\ &\quad \left. + \eta^2 \theta_1^2 e^{2t} (y_{111} z_{111}^2 (5 + 4(2 + \theta_0)z_{111} - 7Fz_{111}^2) - 3) \right), \\ z'_{111} &= \frac{1}{y_{111} z_{111}^2 + \theta_1 e^t (1 + z_{111} + \eta z_{111})} \times \\ &\quad \times \left(y_{111}^2 z_{111}^5 (1 - \eta z_{111} - \theta_0 z_{111} + Fz_{111}^2) \right. \\ &\quad + e^{2t} \theta_1^2 z_{111} (1 + z_{111} + \eta z_{111})^2 (1 - \eta z_{111} - \theta_0 z_{111} + Fz_{111}^2) \\ &\quad \left. + \theta_1 e^t (1 + 2y_{111} z_{111}^3 (1 + z_{111} + \eta z_{111})(1 - \eta z_{111} - \theta_0 z_{111} + Fz_{111}^2)) \right). \end{aligned}$$

In this chart, there are no base points on the exceptional line \mathcal{L}_{10} .

The energy (2.6) is:

$$\begin{aligned} E &= \frac{1}{z_{111}^2} + \frac{\theta_1 e^t - \eta}{z_{111}} + F + (1 - \theta_0)\theta_1 e^t + e^t \theta_1 (F - (1 + \eta)(\eta + \theta_0))z_{111} \\ &\quad + (1 + \eta)\eta e^t F \theta_1 z_{111}^2 + y_{111} z_{111} - (\eta + \theta_0)y_{111} z_{111}^2 + Fy_{111} z_{111}^3. \end{aligned}$$

Second chart:

$$\begin{aligned} y_{112} &= y_{101} - (1 + \eta)\theta_1 e^t = (y - 1)^3 z^2 - (y - 1)z\theta_1 e^t - (1 + \eta)\theta_1 e^t, \\ z_{112} &= \frac{z_{101}}{y_{101} - (1 + \eta)\theta_1 e^t} = \frac{1}{(y - 1)^4 z^3 - (y - 1)^2 z^2 \theta_1 e^t - (y - 1)z(1 + \eta)\theta_1 e^t}, \\ y &= 1 + \theta_1 e^t y_{112} z_{112} + (1 + \eta)\theta_1 e^t y_{112}^2 z_{112}^2 + y_{112}^3 z_{112}^2, \\ z &= \frac{1}{\theta_1 e^t y_{112}^2 z_{112}^2 (1 + (1 + \eta)y_{112} z_{112} + y_{112}^2 z_{112})}. \end{aligned}$$

The Jacobian and its derivative are:

$$\begin{aligned}
J_{112} &= -\theta_1 e^t z_{112} - (1 + \eta)\theta_1 e^t y_{112} z_{112}^2 - y_{112}^2 z_{112}^2, \\
J'_{112} &= 2y_{112}^4 z_{112}^3 ((\eta + \theta_0)y_{112} z_{112} - 1 + Fy_{112}^2 z_{112}^2) \\
&\quad + \theta_1 e^t z_{112} (1 + \eta - (1 + \eta)^2 y_{112} z_{112} - 3y_{112}^2 z_{112} + 4(\theta_0 - 1)y_{112}^3 z_{112}^2 \\
&\quad\quad + 5(\eta + \eta^2 - F + \theta_0 + \eta\theta_0)y_{112}^4 z_{112}^3 - 6F(1 + \eta)y_{112}^5 z_{112}^4) \\
&\quad + \theta_1^2 e^{2t} z_{112} (1 + (1 + \eta)^3 z_{112} + (3 + \eta - 2\theta_0)y_{112} z_{112} \\
&\quad\quad + 2(1 - \eta - 2\eta^2 + 2F - 3\theta_0(1 + \eta))y_{112}^2 z_{112}^2 \\
&\quad\quad - 2(1 + \eta)(2(\eta + \theta_0)(1 + \eta) - 5F)y_{112}^3 z_{112}^3 + 6F(1 + \eta)^2 y_{112}^4 z_{112}^4).
\end{aligned}$$

The exceptional line is $\mathcal{L}_{10} : y_{112} = 0$, while the proper preimage of \mathcal{L}_9 is $z_{112} = 0$. \mathcal{L}_8 is not visible in this chart.

The vector field (2.2) is:

$$\begin{aligned}
y'_{112} &= \frac{2y_{112}^2 z_{112} + \theta_1 e^t (1 + 2(1 + \eta)y_{112} z_{112})}{z_{112}(y_{112}^2 z_{112} + \theta_1 e^t (1 + (1 + \eta)y_{112} z_{112}))} + \frac{(1 + \eta)\theta_1 e^t ((1 + \eta)\theta_1 e^t + y_{112})}{y_{112}^2 z_{112} + \theta_1 e^t (1 + (1 + \eta)y_{112} z_{112})} \\
&\quad - (1 + \eta)^2 \theta_1 e^t - 2Fy_{112}^5 z_{112}^3 - \eta y_{112} + \theta_1^2 e^{2t} y_{112} z_{112} (\eta + \eta^2 - F + \theta_0 + \eta\theta_0) \\
&\quad + \theta_1 e^t y_{112}^2 z_{112} (\eta + \theta_0) + e^{2t} \theta_1^2 (1 + \eta) y_{112}^2 z_{112}^2 (\eta + 2\eta^2 - 3F + \theta_0 + \eta\theta_0) \\
&\quad + (\eta + \theta_0) y_{112}^4 z_{112}^2 - 4e^t F \theta_1 (1 + \eta) y_{112}^4 z_{112}^3 + \theta_1 e^t y_{112}^3 z_{112}^2 (2\eta + 2\eta^2 - 3F + 2\theta_0 + 2\eta\theta_0) \\
&\quad - 2e^{2t} F \theta_1^2 (1 + \eta)^2 y_{112}^3 z_{112}^3, \\
z'_{112} &= \frac{1}{y_{112}^2 z_{112} + \theta_1 e^t (1 + (1 + \eta)y_{112} z_{112})} \times \\
&\quad \times (-3(1 + \eta)\theta_1 e^t z_{112} + (1 + \eta)^3 \theta_1^2 e^{2t} z_{112}^2 - 2y_{112} z_{112} + (1 + \eta)^2 \theta_1 e^t y_{112} z_{112}^2) \\
&\quad + (\eta + \theta_1 e^t) z_{112} - e^{2t} \theta_1^2 (\eta + \eta^2 - F + \theta_0 + \eta\theta_0) z_{112}^2 \\
&\quad + \theta_1 e^t y_{112} z_{112}^2 (1 - \eta - 2\theta_0) - (1 + \eta) e^{2t} (\eta + \eta^2 - 3F + \theta_0 + \eta\theta_0) \theta_1^2 y_{112} z_{112}^3 \\
&\quad + y_{112}^2 z_{112}^2 + \theta_1 e^t y_{112}^2 z_{112}^3 (4F - 3(\eta + \theta_0)(1 + \eta)) + 2(1 + \eta)^2 e^{2t} F \theta_1^2 y_{112}^2 z_{112}^4 \\
&\quad - 2(\eta + \theta_0) y_{112}^3 z_{112}^3 + 5F \theta_1 (1 + \eta) e^t y_{112}^3 z_{112}^4 + 3F y_{112}^4 z_{112}^4.
\end{aligned}$$

There are no base points on the exceptional line \mathcal{L}_{10} in this chart.

The energy (2.6) is:

$$\begin{aligned}
E &= \frac{1}{y_{112}^2 z_{112}^2} + \frac{\theta_1 e^t - \eta}{y_{112} z_{112}} + F + \theta_1 e^t (1 - \theta_0) + y_{112} + \theta_1 e^t (F - (1 + \eta)(\eta + \theta_0)) y_{112} z_{112} \\
&\quad - (\eta + \theta_0) y_{112}^2 z_{112} + (1 + \eta) e^t F \theta_1 y_{112}^2 z_{112}^2 + F y_{112}^3 z_{112}^2.
\end{aligned}$$

APPENDIX B. NOTATION

In this appendix, we collect the notation for base points, provide the charts in which they are defined and their coordinates in these charts, and give the relationships between constants used in the paper.

base point	coordinate system	coordinates
a_0	$(y_{02}, z_{02}) = \left(\frac{1}{y}, \frac{z}{y}\right)$	$(0, 0)$
a_1	$(y_{03}, z_{03}) = \left(\frac{y}{z}, \frac{1}{z}\right)$	$(0, 0)$
a_2	$(y_{12}, z_{12}) = (y_{02}, \frac{z_{02}}{y_{02}}) = \left(\frac{1}{y}, z\right)$	$(0, 0)$
a_3	$(y_{21}, z_{21}) = \left(\frac{y_{03}}{z_{03}}, z_{03}\right) = \left(y, \frac{1}{z}\right)$	$(0, 0)$
a_4	$(y_{21}, z_{21}) = \left(\frac{y_{03}}{z_{03}}, z_{03}\right) = \left(y, \frac{1}{z}\right)$	$(1, 0)$
a_5	$(y_{31}, z_{31}) = \left(\frac{y_{12}}{z_{12}}, z_{12}\right) = \left(\frac{1}{yz}, z\right)$	$\left(\frac{2}{\theta_0 + \eta + \theta_\infty}, 0\right)$
a_6	$(y_{31}, z_{31}) = \left(\frac{y_{12}}{z_{12}}, z_{12}\right) = \left(\frac{1}{yz}, z\right)$	$\left(\frac{2}{\theta_0 + \eta - \theta_\infty}, 0\right)$
a_7	$(y_{41}, z_{41}) = \left(\frac{y_{21}}{z_{21}}, z_{21}\right) = \left(yz, \frac{1}{z}\right)$	$(\theta_0, 0)$
a_8	$(y_{52}, z_{52}) = \left(y_{21} - 1, \frac{z_{21}}{y_{21} - 1}\right) = \left(y - 1, \frac{1}{(y-1)z}\right)$	$(0, 0)$
a_9	$(y_{91}, z_{91}) = \left(\frac{y_{52}}{z_{52}}, z_{52}\right) = \left((y-1)^2 z, \frac{1}{(y-1)z}\right)$	$(\theta_1 e^t, 0)$
a_{10}	$(y_{101}, z_{101}) = \left(\frac{y_{91} - \theta_1 e^t}{z_{91}}, z_{91}\right)$ $= \left((y-1)z((y-1)^2 z - \theta_1 e^t), \frac{1}{(y-1)z}\right)$	$((1 + \eta)\theta_1 e^t, 0)$

Note that the constants used throughout the paper are related as follows.

$$\begin{aligned}\theta_\infty^2 &= 2\alpha, \\ \theta_0^2 &= -2\beta, \\ \theta_1^2 &= -2\delta \quad (\theta_1 \neq 0), \\ \eta &= -\frac{\gamma}{\theta_1} - 1, \\ \epsilon &= \frac{1}{2}(\theta_0 + \theta_\infty + \eta), \\ F &= \frac{1}{2}\epsilon(\theta_0 + \eta - \theta_\infty).\end{aligned}$$

REFERENCES

- Andreev, F. V. and A. V. Kitaev. 1997a. *On connection formulas for the asymptotics of some special solutions of the fifth Painlevé equation*, Zap. Nauchn. Sem. S.-Peterburg. Otdel. Mat. Inst. Steklov. (POMI) **243**, no. Kraev. Zadachi Mat. Fiz. i Smezh. Vopr. Teor. Funktsii. 28, 19–29, 338 (Russian, with English and Russian summaries); English transl., 1997a, J. Math. Sci. (New York) **99**, no. 1, 808–815.
- Andreev, F. V. and A. V. Kitaev. 1997b. *Exponentially small corrections to divergent asymptotic expansions of solutions of the fifth Painlevé equation*, Math. Res. Lett. **4**, no. 5, 741–759.
- Andreev, F. V. and A. V. Kitaev. 2000. *Connection formulae for asymptotics of the fifth Painlevé transcendent on the real axis*, Nonlinearity **13**, no. 5, 1801–1840.
- Boelen, L., G. Filipuk, C. Smet, W. Van Assche, and L. Zhang. 2013. *The generalized Krawtchouk polynomials and the fifth Painlevé equation*, J. Difference Equ. Appl. **19**, no. 9, 1437–1451.
- Bryuno, A. D. and A. V. Parusnikova. 2012. *Expansions of solutions of the fifth Painlevé equation in a neighborhood of its nonsingular point*, Dokl. Akad. Nauk **442**, no. 5, 583–588 (Russian); English transl., 2012, Dokl. Math. **85**, no. 1, 87–92.
- Clarkson, P. A. 2005. *Special polynomials associated with rational solutions of the fifth Painlevé equation*, J. Comput. Appl. Math. **178**, no. 1-2, 111–129.
- Duistermaat, J. J. and N. Joshi. 2011. *Okamoto's space for the first Painlevé equation in Boutroux coordinates*, Arch. Rational Mech. Anal. **202**, 707–785.
- Dyson, F. J. 1995. *The Coulomb fluid and the fifth Painlevé transcendent*, Chen Ning Yang, Int. Press, Cambridge, MA.
- Gordoa, P. R., N. Joshi, and A. Pickering. 2001a. *Truncation-type methods and Bäcklund transformations for ordinary differential equations: the third and fifth Painlevé equations*, Glasg. Math. J. **43A**, 23–32. Integrable systems: linear and nonlinear dynamics (Islay, 1999).
- Gordoa, P. R., N. Joshi, and A. Pickering. 2001b. *Mappings preserving locations of movable poles. II. The third and fifth Painlevé equations*, Nonlinearity **14**, no. 3, 567–582.

- Howes, P. and N. Joshi. 2014. *Global Asymptotics of the Second Painlevé Equation in Okamoto's Space*, Constructive Approximation **39**, no. 1, 11-41.
- Jimbo, M. 1982. *Monodromy problem and the boundary condition for some Painlevé equations*, Publ. Res. Inst. Math. Sci. **18**, no. 3, 1137-1161.
- Jimbo, M., T. Miwa, Y. Môri, and M. Sato. 1980. *Density matrix of an impenetrable Bose gas and the fifth Painlevé transcendent*, Phys. D **1**, no. 1, 80-158.
- Joshi, N. and M. Radnović. 2016. *Asymptotic Behavior of the Fourth Painlevé Transcendents in the Space of Initial Values*, Constructive Approximation **44**, no. 2, 195-231.
- Kaneko, K. and Y. Ohyama. 2007. *Fifth Painlevé transcendents which are analytic at the origin*, Funkcial. Ekvac. **50**, no. 2, 187-212, DOI 10.1619/fesi.50.187. MR2351213
- Lu, Y. and B. McLeod. 1999a. *Asymptotics of the negative solutions to the general fifth Painlevé equation*, Appl. Anal. **73**, no. 3-4, 523-541.
- Lu, Y. and J. B. McLeod. 1999b. *Asymptotics of the nonnegative solutions of the general fifth Painlevé equation*, Appl. Anal. **72**, no. 3-4, 501-517.
- Lu, Y. and Z. Shao. 2004. *Justification of the existence of a group of asymptotics of the general fifth Painlevé transcendent*, Int. J. Math. Math. Sci. **69-72**, 3821-3828.
- McCoy, B. M. and S. Tang. 1986a. *Connection formulae for Painlevé V functions*, Phys. D **19**, no. 1, 42-72.
- McCoy, B. M. and S. Tang. 1986b. *Connection formulae for Painlevé functions*, Phys. D **18**, no. 1-3, 190-196. Solitons and coherent structures (Santa Barbara, Calif., 1985).
- McCoy, B. M. and S. Tang. 1986c. *Connection formulae for Painlevé functions. II. The δ function Bose gas problem*, Phys. D **20**, no. 2-3, 187-216.
- Olver, F. W. J., D. W. Lozier, R. F. Boisvert, and C. W. Clark (eds.) 2010. *NIST handbook of mathematical functions*, U.S. Department of Commerce, National Institute of Standards and Technology, Washington, DC; Cambridge University Press, Cambridge.
- Ohayama, Y. and S. Okumura. 2006. *A coalescent diagram of the Painlevé equations from the viewpoint of isomonodromic deformations*, J. Phys. A **39**, no. 39, 12129-12151.
- Okamoto, K. 1979. *Sur les feuilletages associés aux équation du second ordre à points critiques fixes de P. Painlevé*, Japan J. Math. **5**, no. 1, 1-79.
- Qin, H. Z. and N. N. Shang. 2006. *Asymptotics of the general fifth Painlevé equation*, Acta Math. Sinica (Chin. Ser.) **49**, no. 1, 225-230 (Chinese, with English and Chinese summaries).
- Sasaki, Y. 2007. *Value distribution of the fifth Painlevé transcendents in sectorial domains*, J. Math. Anal. Appl. **330**, no. 2, 817-828, DOI 10.1016/j.jmaa.2006.07.083. MR2308409
- Schief, W. K. 1994. *Bäcklund transformations for the (un)pumped Maxwell-Bloch system and the fifth Painlevé equation*, J. Phys. A **27**, no. 2, 547-557.
- Shimomura, S. 2011. *Truncated solutions of the fifth Painlevé equation*, Funkcial. Ekvac. **54**, no. 3, 451-471.
- Zeng, Z.-Y. and Y.-Q. Zhao. 2016. *Application of uniform asymptotics to the connection formulas of the fifth Painlevé equation*, Appl. Anal. **95**, no. 2, 390-404.

SCHOOL OF MATHEMATICS AND STATISTICS F07, THE UNIVERSITY OF SYDNEY, NEW SOUTH WALES
2006, AUSTRALIA

E-mail address: nalini.joshi@sydney.edu.au

SCHOOL OF MATHEMATICS AND STATISTICS F07, THE UNIVERSITY OF SYDNEY, NEW SOUTH WALES
2006, AUSTRALIA

E-mail address: milena.radnovic@sydney.edu.au